remote sensing

MDPI

Article,

Monitoring land cover change and disturbance of the Mount Wutai World Cultural Landscape Heritage Protected Area based on Remote Sensing time-series image from 1987 to 2018

Xuyu Bai[1,2,3], Peijun Du* [1,2,3], Shanchuan Guo[1,2,3], Peng Zhang[1,2,3], Cong Lin[1,2,3], Pengfei Tang[1,2,3], Ce Zhang[4]

1. School of Geography and Ocean Science, Nanjing University, Nanjing 210023, China
Baixy26@163.com (X.B.); Dupjrs@gmail.com (P.D.); gsccn@outlook.com (S.G.)
2. Key Laboratory for Satellite Mapping Technology and Applications of Ministry of Natural Resources, and Jiangsu Provincial Key Laboratory for Geographic Information Technology, Nanjing 210023, China
3. Jiangsu Center for Collaborative Innovation in Geographical Information Resource Development and Application, School of Geography and Ocean Science, Nanjing University, Nanjing 210023, China
4. Lancaster Environment Centre, Lancaster University, Lancaster LA1 4YQ, UK

* Correspondence: Dupjrs@gmail.com; Tel.: +86-159-0515-9291

Received: date; Accepted: date; Published: date

Abstract: The contextual-based multi-source time-series remote sensing and proposed Comprehensive Heritage Area Threats Index (CHATI) index are used to analyze the spatial-temporal LULCC and threats in the Mount Wutai World Heritage Area. The results show disturbances such as forest coverage, vegetation conditions, mining area and built-up area in research area change dramatically. And according to the CHATI, although different disturbances have positive or negative influence on environment, as an integrated system it keeps stable from 1987 to 2018. Finally, this research uses linear regression and F-test to mark the remarkable variation of spatial-temporal. In consequence, the threats of Mount Wutai be addressed from macro level and micro level. Although there still have some drawbacks, the effectiveness of threats identification has been tested using field validation, the results are a reliable tool to raise the public awareness of WHA protection and for the governance.

Keywords: world heritage area; protected area; disturbance; time series; spatio-temporal analysis; remote sensing

---

1. Introduction

The world heritage is the site with special historic, scientific, or esthetic qualities, and universal value[1]. It has been widely accepted since it was first raised by the United Nations Educational, Scientific and Culture Organization (UNESCO) in 1972[2]. There are four kinds of world heritage: natural heritage, cultural heritage, mixed heritage and cultural landscape heritage[3]. While natural and mixed heritage are closely related to the environment, cultural heritage seems more independent[4]. Cultural heritage includes tangible cultural heritage such as movable, immovable and underwater cultural heritage and intangible cultural heritage which are treasures of human activities, for instance, oral traditions, performing arts and rituals[5]; these kinds of cultural heritage interact with the natural environment deeply[6]. It is meaningful to place the cultural heritage within the surrounding landscape together, as the pattern and context of this system will influence the function and integrity of the whole ecosystem directly[7]. Thus, the analysis of the World Heritage Area (WHA) should encompass heritage sites and their surrounding landscape.

However, the environment change has posed great disturbance, even threats to WHA's security and raised a number of problems to its sustainable protection in a specific area. For instance, the exceeding tourism may destroy the balance of WHA[8]. Continued urbanization not only causes land resource scarcity but also leads to urban heat island[9], which directly changes the characteristic of the heritage[10]. Large-scale agriculture, mining activity and erosion could also threaten the development of WHA[11]. In other words, monitoring WHA and their surrounding environment at the regional level is a fundamental part of cultural heritage protection.

Moreover, the ecological disturbance can be described as "a case; a physical force, agent, or process, either abiotic or biotic, causing a perturbation (which included stress) in an ecological component or system; relative to specified reference state and system; defined by specific characteristics"[12,13]. As a kind of protected areas, WHA has shown common feature and own unique characteristics[12]. It should be noted that both WHA and the protected areas have suffered serious ecological degradation, which threatens the balance of WHA and the whole ecological system badly[8,14]. For instance, the species' population and their habitat condition decrease sharply in the Great Barrier Reef Marine Park due to the poor management[8]; LULC change caused by urbanization or mining, generates a significant influence on the WHA[15]; the Arabian Oryx Sanctuary in Oman has been deleted from the world heritage list because the oil and gas extraction have occupied almost ninety percentage of its original area[8,16]. The land pressure by urbanization and mining activity lead to complex problems of the ecosystem[17-19]. Meanwhile, social, economic, scientific, and political changes in the protected areas are closely connected to the processes of protection[15,20]. In some developing countries, tourism is the main source of the whole income for the development of the local economy. For instance, Rwanda earns about 200 million US dollars per year from tourists who visiting the Volcanos National Park[8,21].

No matter how pollution derived parameters or Land Use/ Land Cover (LULC) change, the impact of constraint factors on the WHA is a prolonged process[12,22]. On the one hand, there is evidence that human activities such as mining, cutting trees and overuse fossil fuel significantly increase the generation of acid gases and other air pollutants[23-25]. It is obvious that under such an environmental background, the WHA will suffer accumulated damage in the long run[6]. On the other hand, LULC change means degradation or increase for a specific category, it will produce a direct spatial pressure on WHA[26,27]. Population migration, technological development, economic growth, politics and values are the driving forces of LULC change[11,25]. According to the studies based on the pressure state response indicator framework[27], the LULC change has a significant influence on the regional water cycle, environmental quality, biodiversity, productivity and adaptability of terrestrial ecosystem, meanwhile, the density of the built-up area and vegetation cover have also vastly impacted the land eco-security[28-32]. It is certain that the LULCC is a continued and dynamic process. Therefore, exploring the impact of LULC in WHA from a time series perspective is quite useful to understand the process comprehensively.

Remote sensing (RS) techniques have revolutionized the traditional recording and prospection approach[7]. By adopting such well-established techniques, the measurement of geographic units becomes more efficiently and detailed[33]. Firstly, RS techniques could provide significant data support for environmental assessment, planning, modelling and prediction[34]. For instance, RS image classification could use medium or high spatial resolution image data and various classifiers including support vector machine, rotation forest and multi-classifier to obtain the LULC information[35-37]. In order to achieve a comprehensive analysis of the dynamic changes of the WHA environment and its driving factors, time series RS products could illustrate the changing process and mechanism[38]. Furthermore, RS techniques could calculate and simulate a plenty of key environmental indicators including chlorophyll a[39], suspended solids concentration[40,41], surface radiance energy budget[42,43], surface moisture and temperature changes[44,45], vegetation cover and land degradation[46,47], vegetation biomass[48,49] and net primary production (NNP)[50,51], vegetation structure[52,53] and ecological parameters[51,54], surface ecological process[55], land use and agricultural vegetation extraction, land cover vegetation ecological process[56-61].

In terms of the RS assessment systems of protected area, there are several frameworks based on different method. Firstly, the system based on PCA (principle component analysis), for instance, RSEI (remote sensing based ecological index) conducted greenness, dryness, wetness and heat four main indicator of ecological then (PCA) was utilized to compress the four indicators into one in order to assess overall regional ecological status[62]. Secondly, system based on weights which come from experiment or experts, such as the applications in groundwater potential zones[63], human settlement environment[18,64,65], mix research in environment and society,[66-68]etc. Then, the system based on pattern recognition methods, such as hierarchy analysis (HA), analytic hierarchy process (AHP), fuzzy evaluation (FE), genetic algorithm (GA), and statistical learning (SL),[65,69-72] etc.

In conclusion, RS assessment systems could be an efficient method to monitor the protected areas. In terms of research objective, according to reference[11], it has been divided into four categories: habit mapping and change detection, the assessment of the habitat degradation, the evaluation of species' diversity and distribution and the track of pressures and threats. Up to now, there are several large numbers of RS assessment systems has been established to monitor protected areas[58,73-75]. There are several assessment systems for different purposes, however, they follow a similar structure, which consists initially on detecting disturbances in the protected areas. These disturbances can be disturbances identification, extraction indicators and assessment. For instance, firstly, disturbances identified in protected areas generally include urbanization, road, construction, mining, logging, agriculture, fire, alien species, hunting, grazing and drought. Secondly, extraction indicators derived from remote sensing datasets have expressed disturbances to the WHA or the eco-system. Then, the assessment framework can be constructed to measure the pressures and threats that influence the protected areas. Although most WHAs have archaeological value, there is no doubt that the protection of WHAs is imperative and urgent[76].

This paper focus on one specific WHA and seeks to identify pressures and disturbances within it, aiming to better understand the interaction between WHA and the surrounding environments. To conduct the research, a comprehensive assessment framework of WHA is proposed, which analyzes the pressures and threats from every single aspect and overview perspective. Based on human activities and natural environment of the selected WHA, four potential disturbances (forest coverage, vegetation condition, built-up area and mining area) are mainly considered in the assessment. To assess the WHA at a regional level, this paper has adopted a synthetic pressure assessment method which integrates three key indicators (land stress, vegetation coverage and water network denseness) and biological richness derived from LULC. Meanwhile, the time series analysis has been successfully employed in describing and mapping the spatio-temporal evolution of disturbances and WHA threats from 1987 to 2018. As the disturbances of WHA have differences in spatial-temporal levels, to comprehensively identify the characteristics of spatial-temporal variation and distribution, the linear regression analysis combined F-test method has been adopted. There are serval researches focus on Mount Wutai environment, but few of them were based on time-series remote sensing technique. This research monitors both LULCC and disturbances of Mount Wutai by adopting remote sensing technique, and proposes a unique index (CHATI) to comprehensively assess the threats of research area. In addition, as we mentioned a lot of RS assessment system has been employed in environment assessment, however, few of them only use RS indicators, that reduce the data dependency in the accepted error range. Furthermore, in this research the spatial temporal analysis is based on linear regression and F-test, which provides more detailed information of spatial variation.

2. Study area and data

2.1. Study area

Mount Wutai, located in southeastern Shanxi Province, China, has a very unique geological structure, magnificent natural scenery, and abundant cultural significance. It mainly consists of two parts: Taihuai Proposed Core Area (N 39°01′50″, E 113°33′48″) and Foguang Proposed Core Area (N 38°52′56″, E 113°20′58″); and the core area has reached 18,415 hectares, which is composed of a series of mountains. The lowest elevation of Wutai Mountain is only 624 meters, while the Beitai Ding is known as "the Roof of North China", with an altitude of 3,061m above sea level. The unique geological structures, stratigraphic profiles, fossil relics of palaeontology, Cenozoic planation and periglacial landforms in the early stage of the earth are perfectly preserved in Mount Wutai. On the mountain, the temperature is relatively low so that the snow covers the high peaks for years. So, it is hard to identity the landscape in winter by RS. The natural resources are well protected, and 8.66% of the mountain is covered with forests with vertical pines, firs, poplars, willow trees, and lush grassland. The pleasant climate and beautiful scenery attract countless tourists and artists[77-79]. As one of the four sacred Buddhist mountains in China, it was affirmed as a UNESCO World Landscape Heritage Site in 2009. It is considered as the bodhimanda of Manjusri (Wenshu in Chinese), who is the Bodhisattva of wisdom. It is said that Buddhism was introduced to Mount Wutai in the Eastern Han Dynasty. Since then, it has become one of the most important centers for the development of Buddhism and has made significant contributions to the development of the Buddhist culture. [77-82].

With the development of economy, human activities play more and more important role in local environment. As Mount Wutai has abundant tourism and mineral resources, the development of tourism and mineral industry has become the focus of local economy. Here just take the development of tourism as the example. Since 1982, Mount Wutai was affirmed as national scenic sports by the State Council, the local government had adopted a series of measures to develop tourism, which including strengthened the construction of tourism infrastructure and built relative tourism supporting service system that integrates food, housing, transportation, travel, shopping and entertainment[83]. The policy of prioritizing tourism had achieved remarkable economic benefits. Until 2008, a total of 2.8102 million domestic and foreign tourists were received the whole year, and the total income of tourism reached 1.405 billion yuan[84]. Over the past three years, the number of tourist receptions had continued to rise, with an average of more than 4 million per year. It can be said that the revenue from tourism and mineral industry has already supports half of the local government's financial benefits[85]. However, such tourism activities, construction of tourism infrastructure and developments of mineral industry have already seriously affected the local ecological environment, such as the variation of the forest coverage. The influences of human activities on the study area will be analyzed in detail by adopting the Remote Sensing techniques.

UNESCO demarcates Mount Wutai into core zone and buffers zone. The Taihuai Proposed Core Zone refers to the area centered around the temple ensemble at the Taihuai Town and the five terrace tops of Mount Wutai. The Proposed Buffer Zone is the protected areas of Mount Wutai. To identify the landscape and threats of Mount Wutai, the research area is demarcated by administration boundary and mountain ridges (as shown in Figure 1). A total area of the research area is about 4781.8km^2.

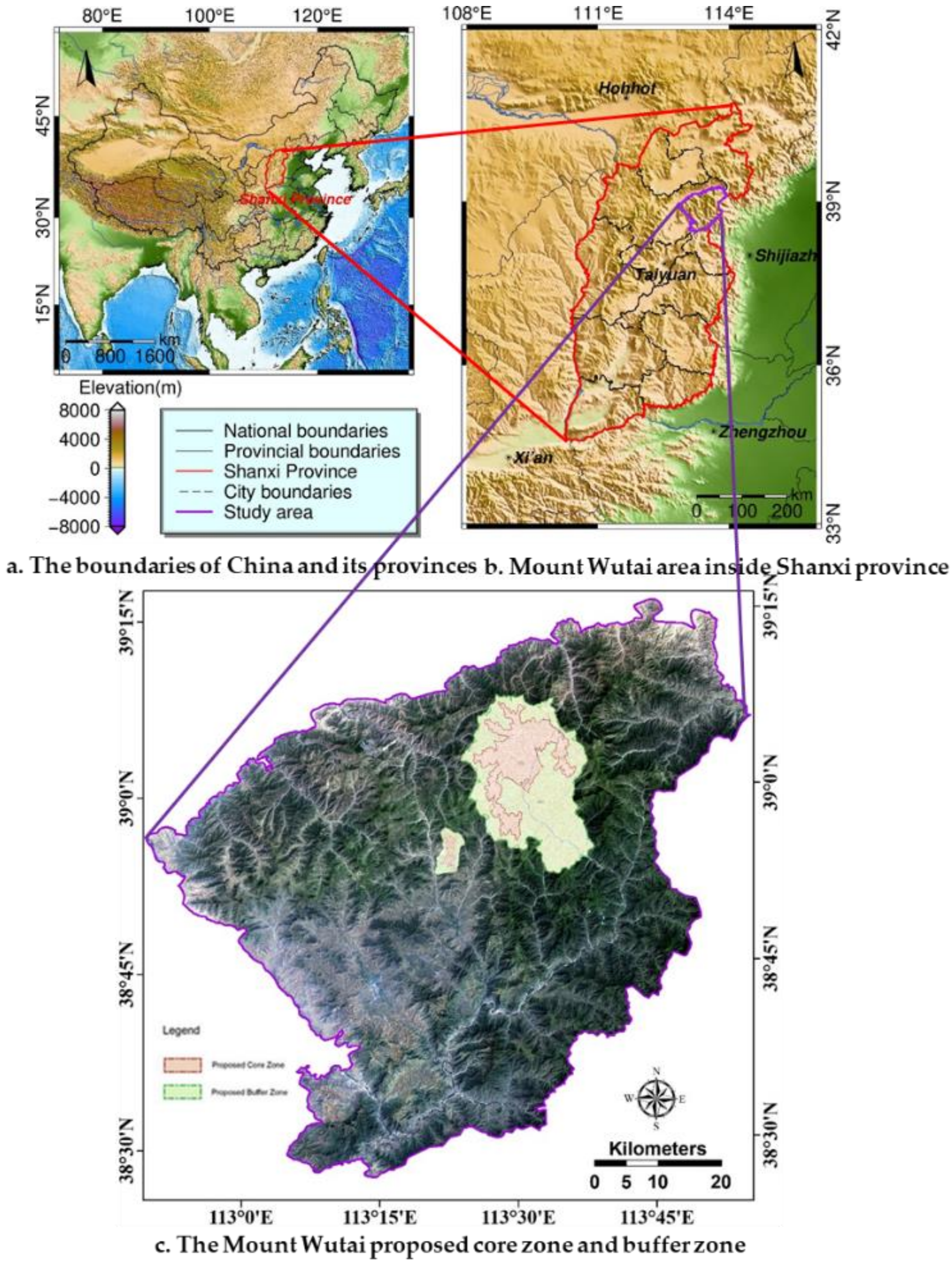

Figure1. Mount Wutai and research area

2.2. Data

This research uses multi-source and multi-temporal data. Firstly, The Modis NDVI products (MOD13Q1) generated by NASA are used to identify the seasonal variation of vegetation coverage and growth situation, 431 phase Modis NDVI products images from 2000 to 2018 with 250-meter spatial resolution and 16 days temporal resolution have been used to derive the mean NDVI value over Mount Wutai (Figure 2). Such results provide guidance to the image selection of Landsat data.

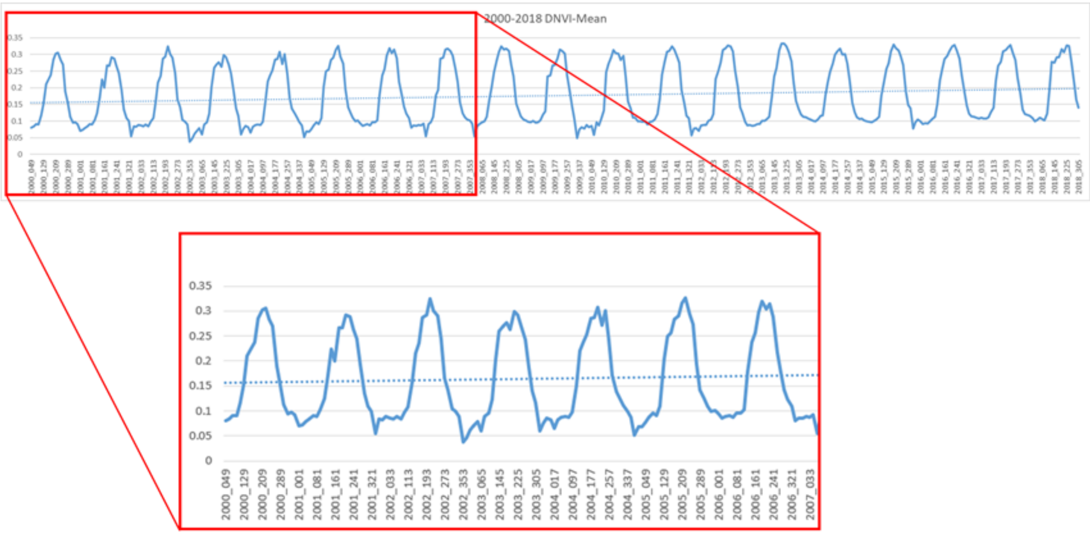

Figure 2. Mean NDVI of Mount Wutai from 2000 to 2018 based MODIS

Secondly, the main data in this research are Landsat time-series data. Those data captured from 1987 to 2018 by Landsat sensors, mainly including TM and OLI images with 30-meter spatial resolution and less than 90% cloud cover (based on a visual estimate). According to the mean NDVI of mount Wutai from 2000 to 2018 (Figure 2.) resulted from Modis NDVI products, regular patterns of seasonal dynamic are shown in the research area. Thus, the data during vegetation growing season from June to September are considered as the best choice to observe the situation of vegetation situation. However, as some years such as 1995, 1998 and 2018 cannot obtain cloud-free Landsat data during that time, we choose adjacent months data. In addition, to show the changes in significance, we choose data every 2 years. Overall, totally 12 phase data are shown in Table 1.

Table 1. The Landsat TM/OLI data from 1987 to 2018

	Jan	Feb	Mar	Apr	May	June	July	Aug	Sept	Oct	Nov	Dec
2018											OLI	
2016									OLI			
2013						OLI						
2010									TM			
2007									TM			
2004						TM						
2001							TM					
1998											TM	
1995					TM							
1992							TM					
1989									TM			
1987									TM			

Thirdly, slope data and aspect data generated by ASTER DEM with 30-meter spatial resolution are used as ancillary data to improve the classification accuracy.

Finally, 1: 100,000 topographic map data, forest resources inventory data were collected from 2016 to 2017 are used in field survey.

All TM/OLI data are processed by ENVI and ArcGIS software. During the image preprocessing period, radiometric calibration is used to eliminate the error of the sensor itself and determine the exact radiation value at the sensor; and atmospheric correction is adopted to eliminate errors caused by atmospheric scattering, absorption and reflection. Geometric correction is employed to eliminate the effects of terrain or deformation caused by camera orientation, mosaic and subset.

3. Method

Long-term time series data have proven to be useful in detecting LULCC, and the subsequent environmental modelling across the regional and global scales[86-88]. And some previous researches have successfully use time-series data in the protected areas[11,89-91]. In the research, 12 phases TM/OLI from 1987 to 2018 are the main time series dataset. Based on the indexes (NDVI, NDSI, MNDWI) and LULC data derived from Landsat time-series data in Mount Wutai, this paper identifies the potential risks and major disturbances of the WHA including biological abundance, land stress degree, vegetation coverage and water network density, and the threat is assessed comprehensively. Firstly, GIS and RS techniques are combined with multi-source data to extract those key factors from Landsat time-series imagery. Secondly, the typical characteristics of the heritage site are analysed from a single factor perspective, then a comprehensive evaluation system and the long-term sequence framework are established. The comprehensive risk of the heritage site is further evaluated. Finally, the result of single factors, such as the vegetation, and comprehensive evaluation are carried out across the perspective of spatial and temporal scales and the changes in the heritage site are analysed throughout the micro and macro scales. The overall method is shown in Figure 3.

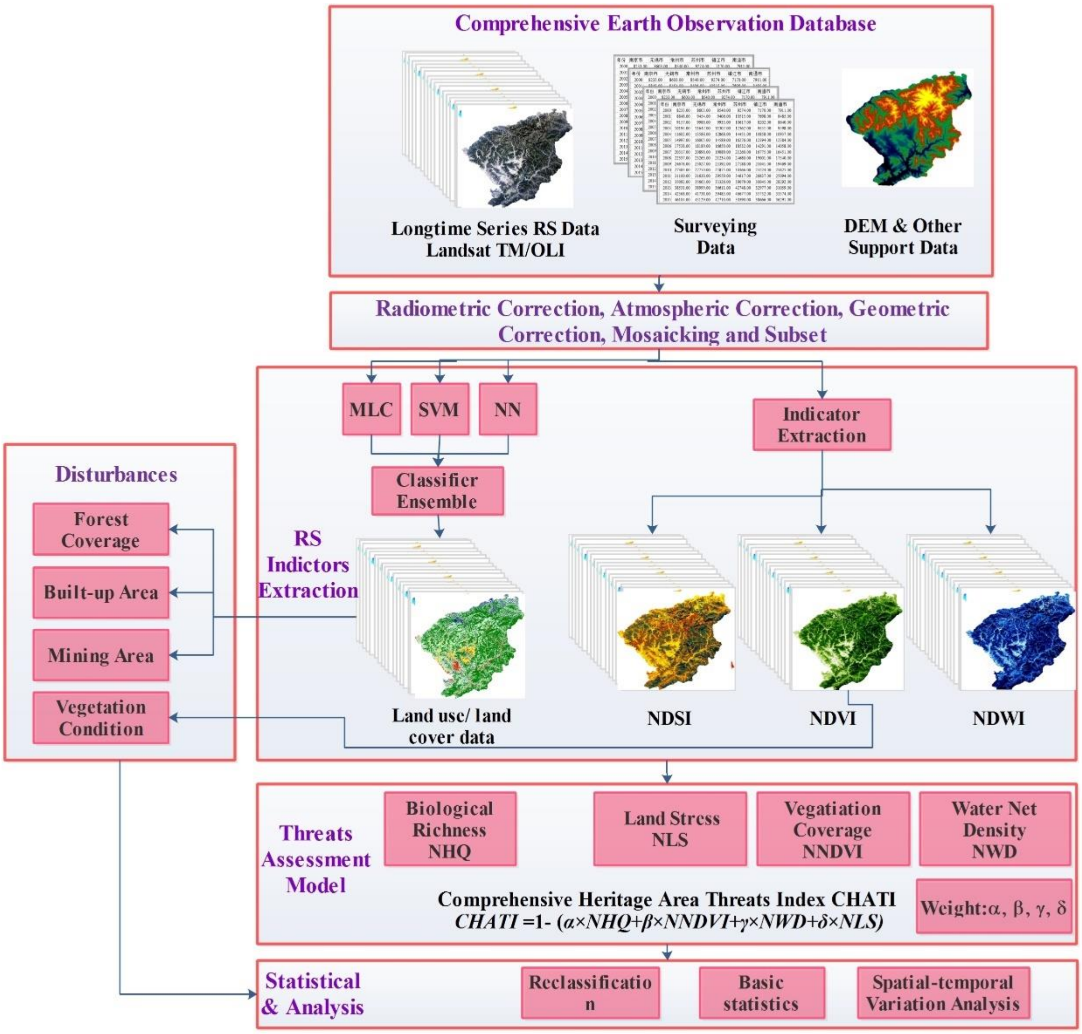

Figure 3. The technical framework

3.1. LULC and indices extraction

The LULC and indices (NDVI, NDSI and MNDWI) are the fundamental baseline data of this research. They are partially the key elements of land cover disturbances identification, and will all contribute to the comprehensive assessment framework. As shown in Figure 3, the LULC is derived from multi-source data, which includes the following steps; 1) selected Landsat data based on seasonal variation of vegetation coverage and growth situation, which statistics from Modis NDVI products in Mount Wutai; 2) making a radiometric correction, atmosphere correction, geometric correction and subset; 3) combining the ASTER DEM, slope data and aspect data with all bands of processed Landsat time-series data; 4) using 3 different single classifier Maximum Likelihood Classification (MLC), Neural Net Classification (NN) and Support Vector Machine Classification (SVM) to achieve 3 LULC classification results for each selected year, the classifications are able to differentiate 7 LULC categories: forest, grass, farmland, building, mining, soil and water. Based on validation, the SVM, MLC and NN shows a good accuracy in green space, building and bared soil in the study area. The 3 LULC classification results are fed into a classifier ensemble, where a simple majority or weight voting is chosen as the ensemble method, the ensemble classifier is the most suitable approach to capture multi-source and complementary information within each individual classifier, which is with the same principle of Random Forest classifier with respects to single decision tree[35]. A classification accuracy assessment is made to validate the results rigorously.

The main indices used in this paper are NDVI, NDSI and MNDWI. NDVI (Normalized difference vegetation index) is the ratio parameter of the near-infrared band (NIR) and infrared band (R) reflectance of remote sensing images. MNDWI (Modified Normalized Differences Water Index) is developed from NDWI[46], which can effectively extraction water information from remote sensing images. NDSI (normalized soil index) is developed from Soil Index (SI), where SI (Soil index) is combined with IBI (index based building index), and uses SAVI (soil-adjusted vegetation index) to exclude the vegetation influence. Consequently, NDSI is the suitable indicator for the building area and bared soil. The comprehensive detail of the indices (equations and further explanations) are listed in Table 2.

Table 2. The indices and explanations

Index	Equation	Variables Explain	References	Number
NDVI	$NDVI = (NIR - R)/(NIR + R)$	NIR: near-infrared band R: infrared band MIR: mid-infrared band BLUE: blue band GREEN: green band SWIR: short-wave infrared band ℓ : soil adjust factor, data range is 0~1, 0 mean extremely high vegetation coverage, contrast 1 is very low. Normally the data is 0.5	[92,93]	1
MNDWI	$MNDWI = \frac{Green - MIR}{Green + MIR}$		[46,94]	2
NSDI	$NDSI = (SI + IBI)/2$		[95-97]	3
SI	$SI = \frac{(MIR + R) - (NIR + BULE)}{(MIR + R) + (NIR + BULE)}$			4
IBI	$IBI = \frac{NDBI - (SAVI + MNDWI)/2}{NDBI + (SAVI + MNDWI)/2}$		[98]	5
SAVI	$SI = \frac{(SWIR - R)(1 + \ell)}{SWIR + R + \ell}$		[99]	6

3.2. Identification of Land Cover Disturbances

Disturbances can be divided into a variety of categories. In general, satellite-based remote sensing focuses on urbanization, road construction, mining, agriculture, fire, invasive species, hunting, grazing and drought. For the Mount Wutai Heritage area, as mentioned in the introduction, the main disturbances covered forest coverage, built-up area, mining area and vegetation conditions. The first three disturbances are derived from LULC data, and the vegetation conditions is characterised by NDVI [53]. Regional statistical approaches are employed to quantify the forest coverage rate, the built-up area and the mining area. The vegetation index is used to characterize the growth of vegetation in the region. According to Zhu (2013)[100], four vegetation indices: normalized difference vegetation index (NDVI), simple ratio Vegetation Index (SR), Modified Normalized Vegetation Index (MNDVI), Reduced Simpler Ratio of Vegetation Index (RSR) are compared in mountainous forests using Landsat TM data. Their research suggests that terrain is strongly influenced ratio vegetation index (RSR and MNDVI); meanwhile, SR and NDVI can largely eliminate the influence of terrain. And NDVI shows a better performance in this area. Therefore, NDVI is selected to characterize the vegetation growth in this study area.

3.3. Comprehensive assessment system of threats in the heritage area.

The comprehensive assessment system of threats in the heritage area is developed from EI (Environment Index), which is constructed according to the "Technical Specifications for Evaluation of Ecological Environment Conditions" of the Ministry of Resources and Environment, China[101], in this system, ecological environment conditions can be evaluated from six aspect: the biological richness, vegetation coverage, water network denseness, land stress, pollution load and environmental restriction. To systemically assess the environment conditions, each of the six aspects developed an index with a corresponding weight. This weight has been published as a guide book. Show as Table 3.

Table 3. The weight of EI

Indicators	Biological Richness Index	Vegetation Coverage Index	Water Network Denseness Index	Land Stress Index	Pollution Load Index	Environmental Restriction Index
Weight	0.35	0.25	0.15	0.15	0.10	Obligatory Target

In terms of the remote sensing assessment, the EECI (Ecological Environment Conditions Index) has been developed.

$$EECI = \alpha \times NHQ + \beta \times NNDVI + \gamma \times NWD + \delta \times NLS \tag{7}$$

This system is focused on the measurable indicators, thus, environmental restriction index will not be considered here. In addition, the pollution load index is characterized by chemical oxygen demand, ammonia nitrogen, sulfur dioxide, dust, nitrogen oxides and solid waste in EI, those indicators show the bearing capacity of the environment for a specific area. Due to those data cannot be effective captured by remote sensing techniques and at some specific areas, the bearing capacities always keeping stable despite some emergency situation. The weight of the pollution load index can be a close to 0. Moreover, in the protected areas, vegetation situation could be more sensitive than another area, thus, the weight of vegetation coverage index can be a trend to 0.35. Finally, the EECI consist of biological richness index, vegetation coverage index, water network denseness index and land stress index. Overall, the coefficients in this equation are similar to EI, α is 0.35, β is 0.35, γ is 0.15 and δ is 0.15.

The NHQ (normalized habitat quality index) is characterized by spatial data after bio-abundance using LULC type reclassification. NNDVI (normalized NDVI) is characterized by normalized vegetation index NDVI. Due to NDVI is extremely sensitive to the surface vegetation and vegetation growth situation. Thus, it is considered as an effective indicator for monitoring regional vegetation and ecological environment changes. The MNDWI has been tested on remote sensing images with different water types, and most of them have achieved better results than NDWI, especially the extraction of water bodies within the urban area. Also, MNDWI can easily distinguish between shadows and water bodies, which solves the difficulty of eliminating shadows in the water extraction problem. NWD (normalized water network deneseness) can be characterized by MNDWI. NLS (the degree of land stress) is the land stress to the environment at the regional level, the stress comes not only from bared soil but also from the built-up area. NDSI combined IBI with SI can avoid the loss of information on construction area by applying SI, in such a case NLS is characterized by NDSI.

In terms of the EECI, high value of EECI indicates the ecological environment conditions is more sustainable and less influenced by the disturbance. Instead, a low value means a high threat in this area. In order to analyze the result consistent with the threat value, the CHATI has been defined as:

$$CHATI = 1 - (\alpha \times NHQ + \beta \times NNDVI + \gamma \times NWD + \delta \times NLS) \quad (8)$$

WHA threat assessment index is the indicator to determine the existing risks of the WHA at the specific time. The value of CHATI is calculated from a lot of spatial variables. The weights for each parameter and indicator come from expert experiences and domain knowledge. According to the weights of EECI and multiple Tests, the final weights are shown in Table 4.

Table 4. Weights of each indicator for calculating CHATI

Parameter	Weight	Indicator			
		Indicator	Weight	LULC	Weight
Biological Richness Index	0.35	BI	0		
		HQ	1	Forest	0.35
				Grass	0.21
				Water	0.28
				Farmland	0.11
				Built-up Area	0.04
				Unused Land	0.01
Vegetation Coverage Index	0.35	NDVI			
Water Network Deneseness Index	0.15	NDWI			
Land Stress Index	0.15	NDSI			

3.4. Variation trends of NDVI and CHATI

As the ecological environmental comprehensive assessment indicators are spatially different, in order to systematically explore the spatial variability and space-time characteristics of the comprehensive ecological environment indicators in the regional level, the method of linear regression analysis[102] + F test[103] is wildly used in the spatial analysis and can provide a reliable results[104-106], with the year as the independent variable. To determine the eco-environmental quality of the CHATI and NDVI indices as dependent variables, a linear regression equation for each pixel is constructed in the study area:

$$\theta_{slope} = \frac{n \times \sum_{i=1}^{n} i \times C_i - \sum_{i=1}^{n} i \sum_{i=1}^{n} C_i}{n \times \sum_{i=1}^{n} i^2 - \left(\sum_{i=1}^{n} i\right)^2} \quad (9)$$

θ_{slope} is the slope of the regression equation for NDVI and CHATI; n is the number of years of the study period (11a for 1987-2018); i is the year number from 1 to 12, and C_i is the NDVI and CHATI sequence data for the study subjects. If θ_{slope} is positive, it indicates that the research object changes with time, and the larger the value, the more obvious the upward trend; otherwise, the research object declines. The significance test of the trend can also be tested. The significance only represents the level of confidence in the trend change and has nothing to do with the speed of change. Its calculation formula is as follows:

$$F = U \times \frac{n-2}{Q} \quad (10)$$

$$U = \sum_{i=1}^{n} \left(\hat{y}i - \bar{y} \right)^2 \quad (11)$$

$$Q = \sum_{i=1}^{n} \left(yi - \hat{y}i \right)^2 \quad (12)$$

In the formula, the ***U*** is sum of the squares of the regression; ***Q*** is the sum of the squares of the errors, in which y_i is the actual observation value of the year, ***i*** and $\hat{y}_i$ is the regression value, which is the average value of 12 years, while $\bar{y}_i$ is the number of years. According to the test results, the trend is divided into the following seven levels: significant decrease (Slope<0, P<0.05); decrease (Slope<0, 0.05<P<0.1); slightly decrease (Slope<0,0.1<P); slightly increase (Slope>0,0.1<P); increase (Slope<0,0.05<P<0.1); significant increase (Slope<0, P<0.05)

4. Result and analysis

4.1. The distribution and variation of main disturbances

Land Use/ Land Cover change based remotely sensed time-series imagery has been widely used in the land resource monitoring and management[107]. This method can select different classification categories depending on the research objectives[108]. We focused on the forest, grass land, mining area, farmland, building, water and bared soil in this research to understand the disturbances in WHA. The LULC maps from 1987 to 2018 are generated by a supervised classifier ensemble as shown in Figure 4.

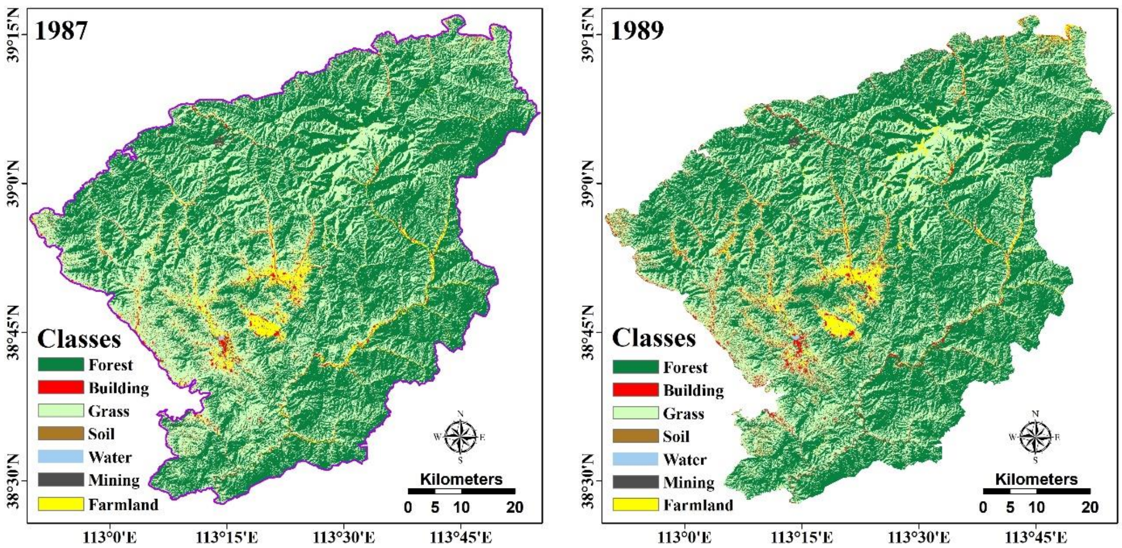

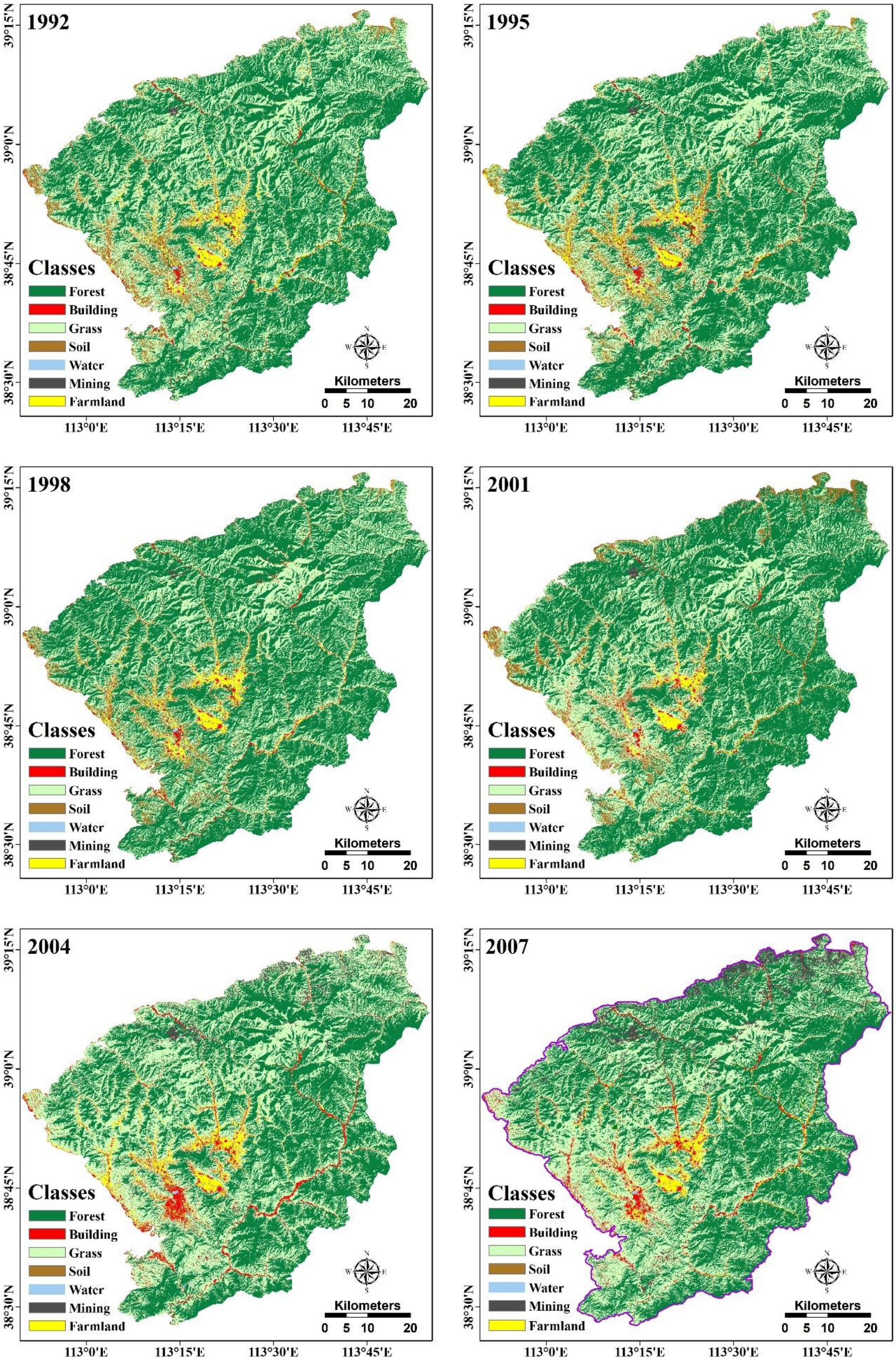
1992
1995
1998
2001
2004
2007
Classes
Forest
Building
Grass
Soil
Water
Mining
Farmland
Kilometers
0 5 10 20
N
S
W
E
39°15'N
39°0'N
38°45'N
38°30'N
113°0'E
113°15'E
113°30'E
113°45'E

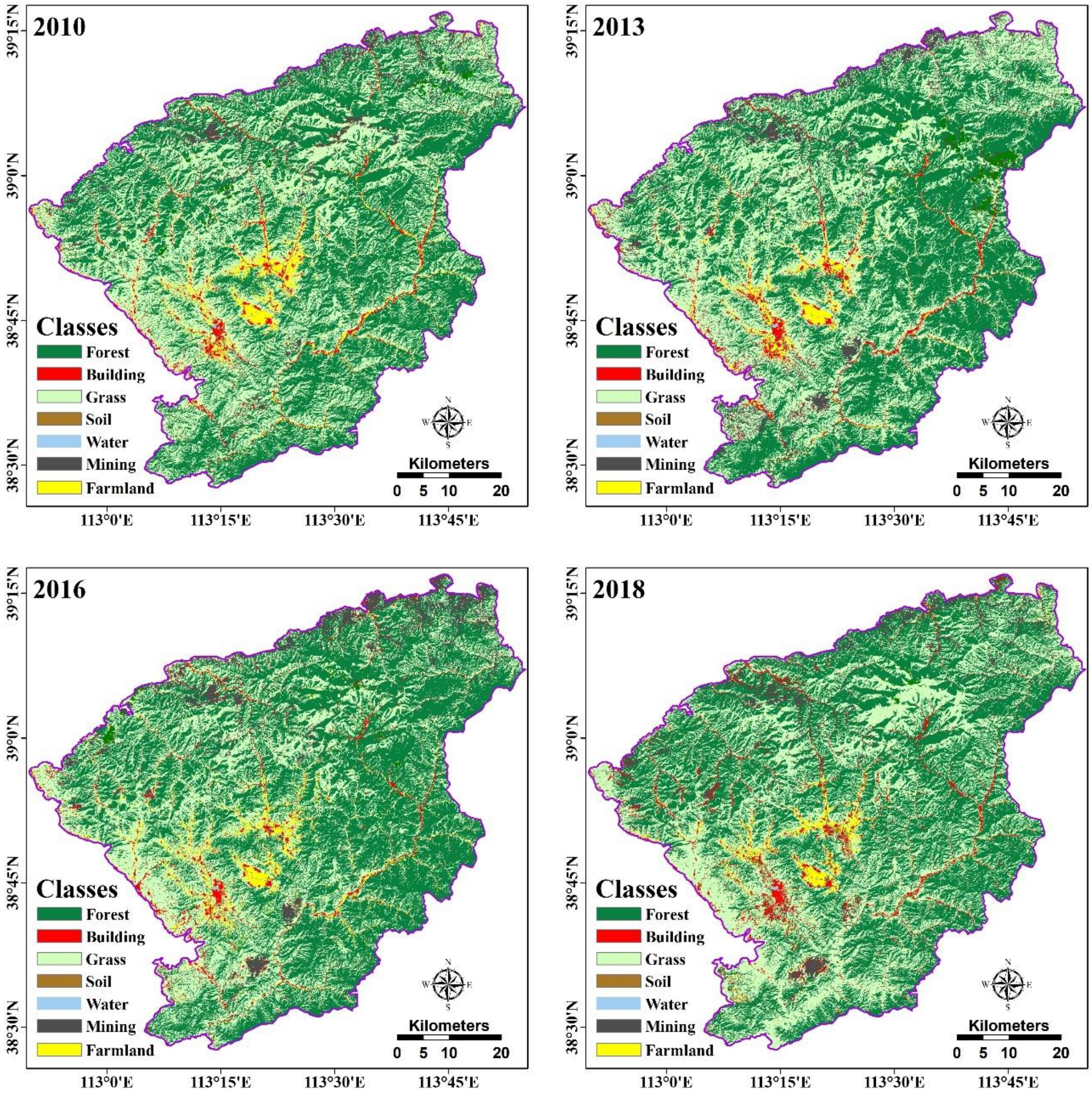

Figure. 4. The Land Use/ Land Cover (LULC) of Mount Wutai from 1987 to 2018

Those LULC maps obtained from remote sensing data are accompanied by a certain error probability[109]. There are many reasons that could lead to error probability, such as the selected classifier (based different algorithms), image quality (cloud coverage, sensors type and so on), training data quality[107]. To assess the classification results, the confusion Matrix including Overall Accuracy (OA) and Kappa Coefficient[110] were adopted in this research (Table 5). From this table, the majority of the OA is over 85% which is considered as the acceptable classification accuracy in the remote sensing applications[111].

Table 5. The accuracy of the classification

Year		1987	1989	1992	1995	1998	2001	2004	2007	2010	2013	2016	2018
Accuracy	Overall Accuracy (%)	90.47	89.99	93.10	86.50	92.90	90.88	95.17	92.83	93.54	93.16	93.89	94.44
	Kappa Coefficient	0.91	0.91	0.92	0.85	0.93	0.90	0.95	0.92	0.93	0.92	0.93	0.94

To better understand the changes between all categories, 11 from-to table that includes the area of the LULC classes for each selected year has been listed (Table 6).

Table 6. The from-to table from 1987 to 2018 for each selected year

Year	1987									
	Classes	FOREST	BUILDING	SOIL	WATER	MINING	FARMLAND	GRASS	Row Total	Class Total
	FOREST	2396.16	3.86	2.68	0.01	13.34	18.21	180.79	2615.05	2615.05
	BUILDING	3.13	46.19	2.38	0.01	1.04	13.64	26.07	92.46	92.46
	GRASS	186.67	18.67	12.73	0.00	5.36	27.42	1542.38	1793.25	1793.25
	SOIL	7.60	1.77	10.25	0.00	0.70	3.07	88.13	111.51	111.51
1989	WATER	0.00	0.20	0.00	0.63	0.03	0.03	0.01	0.90	0.90
	MINING	11.39	3.59	0.83	0.01	15.52	0.11	17.19	48.63	48.63
	FARMLAND	4.99	4.86	3.48	0.00	0.13	65.53	41.02	120.01	120.01
	Class Total	2609.93	79.15	32.34	0.67	36.11	128.00	1895.59	0.00	0.00
	Class Changes	213.77	32.96	22.09	0.04	20.60	62.48	353.21	0.00	0.00
	Image Difference	5.11	13.31	79.17	0.23	12.52	-8.00	-102.34	0.00	0.00

Year	1989									
	Classes	FOREST	BUILDING	GRASS	SOIL	WATER	MINING	FARMLAND	Row Total	Class Total
	FOREST	2233.36	4.41	199.97	4.75	0.02	6.90	12.49	2461.91	2461.91
	BUILDING	6.00	39.83	19.32	2.26	0.07	2.13	4.38	73.99	73.99
	GRASS	345.31	28.19	1435.74	55.08	0.00	23.29	29.64	1917.27	1917.27
	SOIL	9.36	13.08	111.17	45.56	0.00	5.43	20.90	205.50	205.50
1992	WATER	0.00	0.02	0.01	0.00	0.70	0.02	0.00	0.76	0.76
	MINING	12.83	1.37	4.92	0.21	0.10	10.85	0.04	30.33	30.33
	FARMLAND	8.18	5.55	22.11	3.65	0.00	0.01	52.55	92.05	92.05
	Class Total	2615.05	92.46	1793.25	111.51	0.90	48.63	120.01	0.00	0.00
	Class Changes	381.68	52.62	357.51	65.95	0.19	37.78	67.46	0.00	0.00
	Image Difference	-153.14	-18.47	124.02	93.98	-0.13	-18.30	-27.95	0.00	0.00

Year	1992									
	Classes	FOREST	BUILDING	GRASS	SOIL	WATER	MINING	FARMLAND	Row Total	Class Total
	FOREST	2231.62	10.87	286.08	0.97	0.00	8.89	2.91	2541.34	2541.34
	BUILDING	8.17	43.33	35.02	0.98	0.01	1.50	6.35	95.37	95.37
	GRASS	207.95	15.08	1494.72	71.34	0.00	9.99	26.17	1825.26	1825.26
1995	SOIL	2.81	0.35	73.62	109.67	0.00	0.23	14.49	201.17	201.17
	WATER	0.04	0.10	0.08	0.00	0.73	0.18	0.00	1.13	1.13
	MINING	9.78	2.12	6.22	0.04	0.02	9.53	0.00	27.70	27.70
	FARMLAND	1.53	2.15	21.54	22.48	0.00	0.01	42.13	89.84	89.84
	Class Total	2461.91	73.99	1917.27	205.50	0.76	30.33	92.05	0.00	0.00
	Class Changes	230.29	30.66	422.55	95.82	0.03	20.80	49.92	0.00	0.00
	Image Difference	79.43	21.38	-92.01	-4.33	0.36	-2.63	-2.21	0.00	0.00

Year	1995									
	Classes	FOREST	BUILDING	GRASS	SOIL	WATER	MINING	FARMLAND	Row Total	Class Total
	FOREST	2347.97	13.45	359.16	8.52	0.07	17.80	1.21	2748.17	2748.17
	BUILDING	9.44	41.51	21.05	2.56	0.11	1.69	4.38	80.74	80.74
	GRASS	178.22	32.33	1349.20	72.84	0.00	3.42	25.73	1661.74	1661.74
1998	SOIL	1.43	2.17	61.06	98.85	0.00	0.20	14.10	177.81	177.81
	WATER	0.04	0.02	0.01	0.00	0.90	0.09	0.00	1.06	1.06
	MINING	3.39	1.60	14.89	4.27	0.05	4.50	0.04	28.74	28.74
	FARMLAND	0.84	4.29	19.89	14.13	0.00	0.01	44.38	83.54	83.54
	Class Total	2541.34	95.37	1825.26	201.17	1.13	27.70	89.84	0.00	0.00
	Class Changes	193.37	53.85	476.06	102.31	0.23	23.20	45.46	0.00	0.00
	Image Difference	206.83	-14.63	-163.52	-23.35	-0.07	1.04	-6.30	0.00	0.00

Year	1998									
	Classes	FOREST	BUILDING	GRASS	SOIL	WATER	MINING	FARMLAND	Row Total	Class Total
	FOREST	2349.04	4.80	322.17	10.65	0.04	4.55	3.70	2694.95	2694.95
	BUILDING	3.92	35.11	23.53	7.46	0.11	1.50	10.78	82.41	82.41
	GRASS	347.51	25.62	1190.38	78.97	0.04	10.89	21.64	1675.05	1675.05
	SOIL	18.16	9.00	92.24	76.22	0.08	5.40	6.39	207.50	207.50
2001	WATER	0.02	0.06	0.00	0.00	0.74	0.02	0.00	0.84	0.84
	MINING	24.33	0.86	13.38	1.06	0.04	6.35	0.05	46.07	46.07
	FARMLAND	5.19	5.28	20.04	3.46	0.00	0.03	40.98	74.98	74.98
	Class Total	2748.17	80.74	1661.74	177.81	1.06	28.74	83.54	0.00	0.00
	Class Changes	399.13	45.62	471.36	101.59	0.32	22.39	42.56	0.00	0.00
	Image Difference	-53.23	1.67	13.31	29.69	-0.22	17.33	-8.56	0.00	0.00

Year	2001									
	Classes	FOREST	BUILDING	GRASS	SOIL	WATER	MINING	FARMLAND	Row Total	Class Total
	FOREST	2042.90	0.27	129.77	0.14	0.00	4.72	0.35	2178.15	2178.15
	BUILDING	18.38	50.60	62.15	17.86	0.02	1.53	20.48	171.02	171.02
	GRASS	541.38	14.03	1388.67	143.76	0.00	15.47	6.02	2109.34	2109.34
	SOIL	0.10	0.13	0.54	0.33	0.00	0.00	0.31	1.41	1.41
2004	WATER	0.35	0.13	1.04	0.87	0.81	0.13	0.01	3.33	3.33
	MINING	86.33	2.29	51.72	24.60	0.01	24.14	0.05	189.14	189.14
	FARMLAND	5.52	14.96	41.15	19.95	0.00	0.07	47.76	129.41	129.41
	Class Total	2694.95	82.41	1675.05	207.50	0.84	46.07	74.98	0.00	0.00
	Class Changes	652.05	31.81	286.38	207.17	0.03	21.93	27.22	0.00	0.00
	Image Difference	-516.80	88.61	434.29	-206.10	2.49	143.07	54.43	0.00	0.00

Year	2004									
	Classes	FOREST	BUILDING	GRASS	SOIL	WATER	MINING	FARMLAND	Row Total	Class Total
	FOREST	1945.77	1.62	219.82	0.00	0.10	41.42	0.30	2209.04	2209.04
	BUILDING	0.68	89.39	25.27	0.36	0.32	2.90	34.86	153.78	153.78
	GRASS	200.14	40.27	1681.88	0.50	0.41	60.72	38.91	2022.82	2022.82
	SOIL	0.01	0.03	0.61	0.00	0.00	0.01	0.02	0.68	0.68
2007	WATER	0.04	0.11	0.08	0.00	0.97	0.08	0.00	1.28	1.28
	MINING	25.05	4.36	161.26	0.01	1.52	82.76	1.15	276.12	276.12
	FARMLAND	6.45	35.25	20.43	0.53	0.00	1.26	54.17	118.09	118.09
	Class Total	2178.15	171.02	2109.34	1.41	3.33	189.14	129.41	0.00	0.00
	Class Changes	232.37	81.63	427.47	1.41	2.36	106.38	75.25	0.00	0.00
	Image Difference	30.89	-17.25	-86.52	-0.73	-2.05	86.98	-11.32	0.00	0.00

Year	2007									
	Classes	FOREST	BUILDING	GRASS	SOIL	WATER	MINING	FARMLAND	Row Total	Class Total
	FOREST	1997.00	1.49	227.64	0.01	0.07	35.69	0.86	2262.76	2262.76
	BUILDING	0.81	93.12	17.25	0.04	0.29	9.74	12.67	133.92	133.92
	GRASS	183.39	33.11	1699.17	0.15	0.04	89.13	17.03	2022.01	2022.01
	SOIL	0.00	0.10	0.10	0.02	0.00	0.10	0.04	0.36	0.36
2010	WATER	0.06	1.60	0.13	0.01	0.70	0.12	0.61	3.22	3.22
	MINING	21.09	2.54	48.52	0.10	0.16	140.80	0.30	213.51	213.51
	FARMLAND	6.69	21.82	30.02	0.36	0.02	0.55	86.57	146.02	146.02
	Class Total	2209.04	153.78	2022.82	0.68	1.28	276.12	118.09	0.00	0.00
	Class Changes	212.03	60.65	323.66	0.66	0.58	135.32	31.52	0.00	0.00
	Image Difference	53.72	-19.86	-0.81	-0.32	1.94	-62.60	27.93	0.00	0.00

Year	2010									
	Classes	FOREST	BUILDING	GRASS	SOIL	WATER	MINING	FARMLAND	Row Total	Class Total
	FOREST	1862.08	1.63	402.00	0.01	0.08	23.11	17.39	2306.30	2309.06
	BUILDING	3.63	71.43	26.15	0.06	1.17	4.76	13.76	120.95	121.18
	GRASS	320.00	34.16	1472.83	0.22	0.30	72.74	53.43	1953.67	1954.03
	SOIL	0.06	0.34	0.59	0.00	0.01	0.01	2.27	3.29	3.29
2013	WATER	0.24	0.36	0.07	0.00	0.66	0.26	0.03	1.61	1.70
	MINING	74.05	16.82	93.22	0.06	0.37	111.71	2.57	298.80	299.33
	FARMLAND	2.25	8.52	25.31	0.01	0.61	0.37	56.42	93.49	93.53
	Class Total	2262.76	133.92	2022.01	0.36	3.22	213.51	146.02	0.00	0.00
	Class Changes	400.68	62.49	549.19	0.36	2.56	101.81	89.60	0.00	0.00
	Image Difference	46.30	-12.74	-67.99	2.93	-1.52	85.82	-52.49	0.00	0.00

Year	2013									
	Classes	FOREST	BUILDING	GRASS	SOIL	WATER	MINING	FARMLAND	Row Total	Class Total
	FOREST	2026.06	6.08	348.59	0.65	0.01	29.35	7.52	2418.26	2419.17
	BUILDING	4.85	56.76	33.22	0.14	0.16	34.68	3.37	133.20	133.47
	GRASS	249.91	34.50	1390.82	1.56	0.02	85.55	35.69	1798.04	1798.73
	SOIL	1.73	1.14	13.33	0.10	0.00	2.02	5.95	24.28	24.28
2016	WATER	0.04	0.07	0.01	0.00	1.01	0.16	0.00	1.30	1.30
	MINING	13.02	12.10	116.16	0.05	0.41	142.12	0.84	284.70	284.87
	FARMLAND	12.02	10.60	50.99	0.78	0.01	4.35	40.30	119.06	119.16
	Class Total	2308.64	121.48	1953.35	3.29	1.72	299.47	93.69	0.00	0.00
	Class Changes	282.58	64.72	562.54	3.19	0.71	157.35	53.39	0.00	0.00
	Image Difference	110.53	11.99	-154.62	20.99	-0.42	-14.60	25.47	0.00	0.00

Year	2016									
	Classes	FOREST	BUILDING	GRASS	SOIL	WATER	MINING	FARMLAND	Row Total	Class Total
	FOREST	2018.30	5.37	176.55	1.80	0.03	42.04	14.59	2258.69	2258.69
	BUILDING	7.41	71.62	49.45	2.22	0.05	24.31	10.36	165.43	165.43
	GRASS	378.97	26.72	1466.82	10.32	0.02	71.97	31.65	1986.47	1986.47
	SOIL	0.23	1.31	7.98	1.68	0.00	0.40	8.73	20.33	20.33
2018	WATER	0.00	0.08	0.05	0.00	1.00	0.25	0.07	1.46	1.46
	MINING	13.00	25.82	70.60	4.17	0.20	141.76	10.44	265.98	265.98
	FARMLAND	1.44	2.71	27.77	4.08	0.00	3.90	43.54	83.45	83.45
	Class Total	2419.36	133.63	1799.23	24.27	1.30	284.63	119.38	0.00	0.00
	Class Changes	401.06	62.01	332.41	22.59	0.30	142.87	75.84	0.00	0.00
	Image Difference	-160.67	31.80	187.24	-3.94	0.15	-18.65	-35.93	0.00	0.00

From the data statistic (Figure 5) and LULC maps, the development of Mount Wutai over 30 years from 1987 to 2018 is demonstrated comprehensively. Overall, forest coverage of Mount Wutai is in decline. On the contrary, building area shows a significant increase. The mining area explosion to a peak point and then slowly decrease. The bared soil shows an increasing trend. Whereas the farmland decreases initially with a slight increase thereafter. Small area of water is found in Mount Wutai, where the area keeps stable. in terms of the grassland, its area fluctuates drastically. Detailed description of each category and disturbances are illustrated as follows.

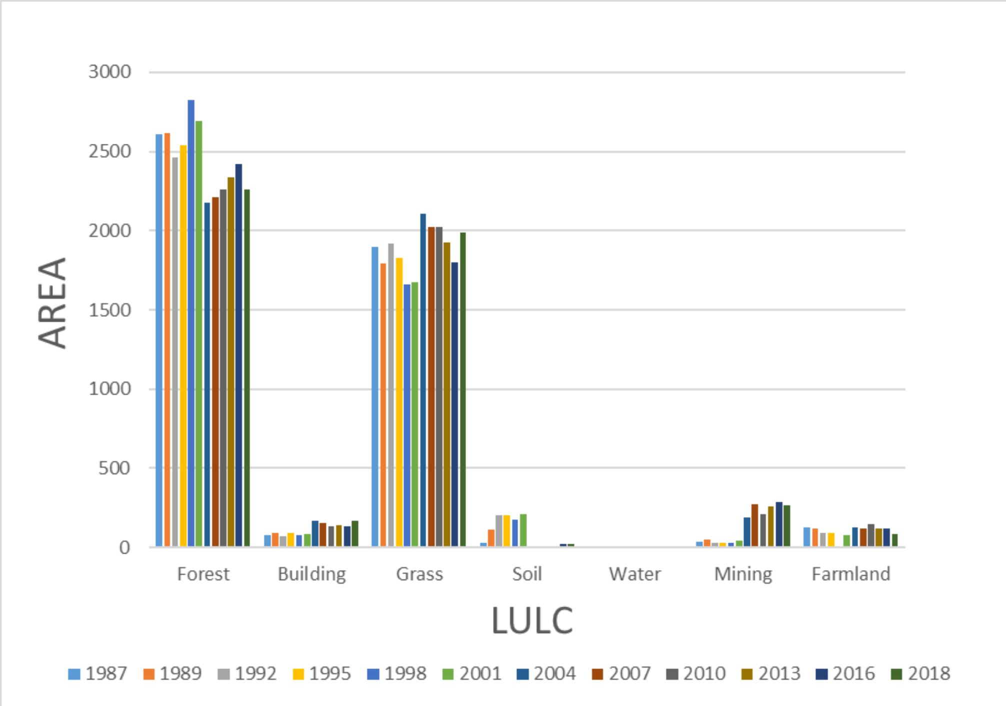

Figure 6. The total area of each LULC categories from 1987 to 2018 (Km²)

Firstly, this paper focus on the four main disturbances of this area which has been identified in the methodology. respectively, forest coverage, vegetation conditions, built-up area and mining area.

Forest coverage is derived from the LULC map. From the macro-perspective, the forest coverage of Mount Wutai has declined in fluctuation. In 1982, Mount Wutai was approved by the State Council to be included in the list of the first batch of national scenic spots[81]. It raised the public's awareness on protecting green vegetation. At the same time, Wutai County was only 0.2 billion RMB Yuan in 1987 according to the references the GDP (Gross Domestic Product)[112], the secondary industry only occupied 14.5%[83], where the majority of people lived in the countryside[112]. Thus, the human activities had a little influence on the environmental of Mount Wutai. The forest coverage remained stable at that time. In 1992, Mount Wutai was becoming a national forest park. Government of Wutai County received the special funds to plant more trees and protect the environmental of Mount Wutai[81], where forest coverage reached a peak point. However, since the 1990s, industrialization has been increasing across the whole Shanxi Province, China[113] (Figure 7). Human activities became the main factor of regional and environmental balance[85]. From the from-to table (Table 6),

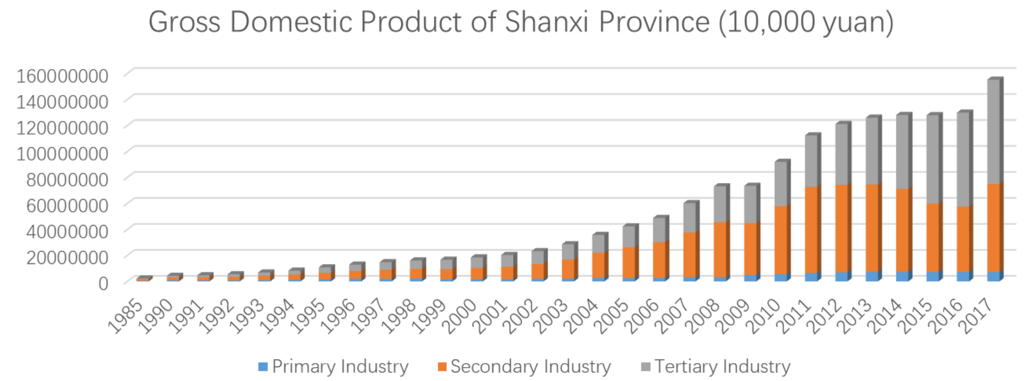

Figure 7. The Gross Domestic Product (GDP) of Shanxi province and Wutai county

some of the forests had been changed into a built-up area or mining area. In 2000, the government of Mount Wutai prepared to apply to be a World Heritage Site[114]. A tree planting program began to show a positive impact of forest coverage. Only in 2017, 3314,863 Hectare trees have been planted in the Mount Wutai area [113]. From the micro perspective, forest in the LULC maps shows an increase around the core protected area of Mount Wutai. The main degradation area is concentrated in built-up area and mining area. It is consistent with the existing literatures[83,112-114].

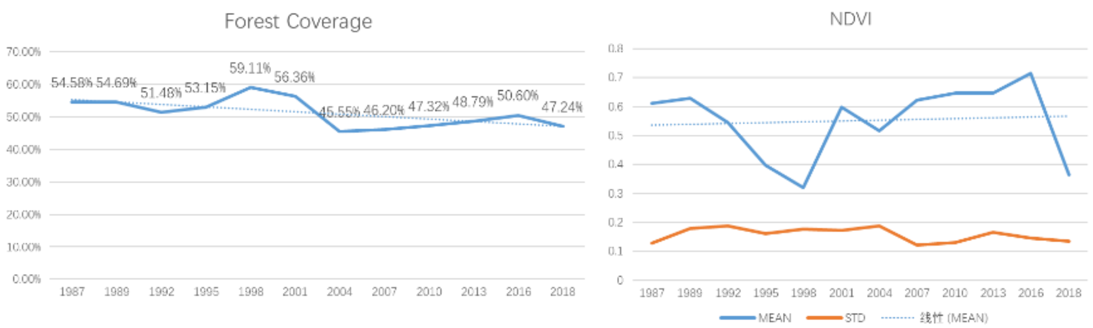

Figure 8. The forest coverage and mean NDVI of Mount Wutai from 1987 to 2018

For the vegetation conditions, there is a large number of remote sensing index has the ability to efficiently and effectively characterise vegetation conditions[46,93,99,100,115], in this paper, NDVIs generated from Landsat images are adopted for each selected year to indicate the vegetation conditions. For entire Mount Wutai, the mean NDVI keeps stable, despite the seasonal effective in 1995, 1998 and 2018 (Figure 8). To identify the spatial variation of vegetation conditions, a significance of variation in NDVI based on F-test shows in Figure 9. This figure can directly show the trend in changes of each pixel. As the figure shows, the vegetation condition significance decreases in the mining area and built-up area, and the slight red line in the map is consistent with the road network that has been built over the last 30 years.

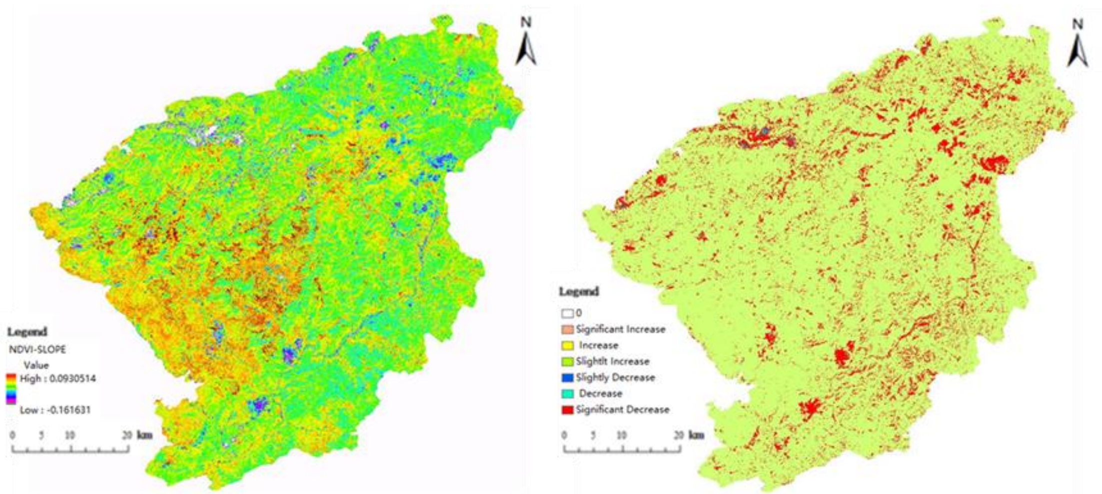

(a)Slope value **(b) Significance of variation**

Figure 9. The spatial distribution of the variation trend of NDVI value 1987-2018 in Mount Wutai

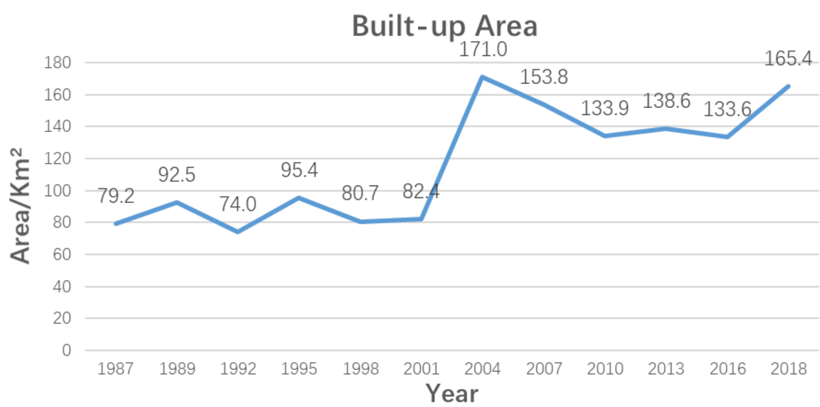

Figure 10. The built-up area of Mount Wutai from 1987 to 2018

Meanwhile, the built-up area fluctuated dramatically as shown in Fig 10. Over the period from 1987 to 2001, the number household in Shanxi province increase at fast pace[84] (Figure 11). However, the urbanization process has not significantly influenced the Wutai county due to the slow economic development, and the area is stable between 50 Km^2 to 100 Km^2. In 1994, central government of China made a decision to reform the urban housing system[116]. This event transferred the urban house system from public housing system into housing market system [117]. After that, crowed real estate companies rush into the province level house market and county level house market[118]. The year 2001-2004 witnesses a sharp rise in the built-up area, and in 2004 the built-up area has become more than 170 Km², for which another reason is because fundamental infrastructure investment sharply increased in the whole Shanxi Province[113] (Figure 12). For Mount Wutai, the total road length increased from 100 Km in 1987 to 1227 Km in 2017[119]. But, after 2004, the population of Mount Wutai area increase slightly[120], due to an increasing number of people migrate to the large cities[121]. In addition, the investment of fundamental infrastructure has also abandoned. the built-up area began returning into a stable stage.

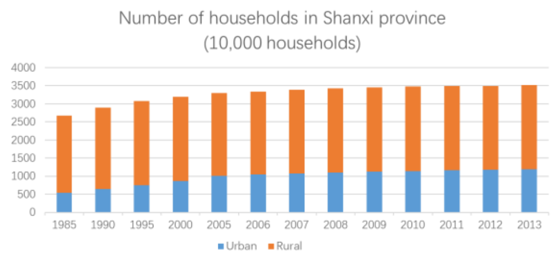

Figure 11. Number of households

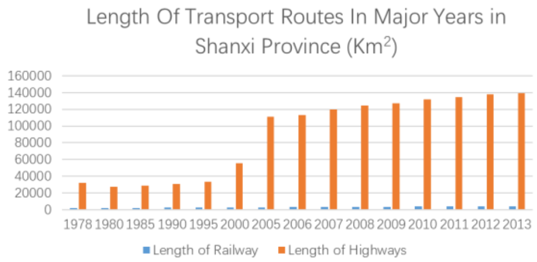

Figure 12. Length of transport routes

Mount Wutai has abundant mineral resources, including 30 kinds of metal and non-metal mineral products, and among them, iron ore and coal most common[112]. Consequently, the exploitation of mineral resources is also an important part of the development in Mount Wutai. From 2011 to 2014, more than half tax from that industry[120] (Table 7). Owing to the limitation of the economy and technology, the mining area

Table 7. The tax from industry in Wutai County from 2011 to 2014

	2011		2012		2013		2014	
	The tax amount	Percentage of all tax	The tax amount	Percentage of all tax	The tax amount	Percentage of all tax	The tax amount	Percentage of all tax
Magnesium industry	1438	5.6%	2007	7.8%	2714	8.6%	1551	4.6%
Coal industry	No data	No data	No data	No data	434	1.4%	5428	15.9%
Electric power industry	4060	25.5%	8080	31.3%	8359	26.5%	1958	7.2%

remains steady from 1987 to 2001 and has not surpassed 50 Km². The year 2001, due to the high demand in coal and iron, all Shanxi Province expand production capacity for industrial production[113](Figure 13), and consequently, the economy of Wutai County developed rapidly[119] (Figure 14), with a fundamental shift towards growing energy markets. The mining area in Mount Wutai expanded dramatically, which is the second reason of the downturn of the forest

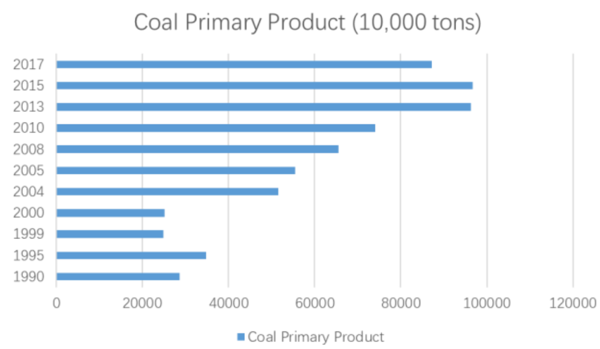

Figure 13. Coal primary product

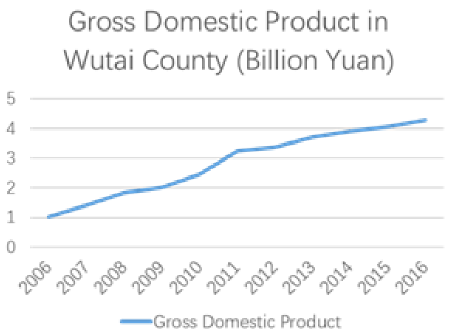

Figure 14. GDP in Wutai county

coverage, and reaches a peak at almost 300 Km^2 in 2007. During that time, a lot of illegal coal mining surface appeared[122,123]. In 2008, the energy market of Shanxi Province has suffered from a cold winter, due to the world economic crisis[124,125]. The development of mining areas tends to be stable. During the following three years, the mining area has a small amount of decline. Since 2010 to 2016, the state government processed the coal company reorganization and resource product optimizing programme[126], this programme aims to optimize allocation of resources and improve safety system. Most of the illegal mining sites has been shut down. Since that, it begins to develop in a stable stage (Figure 15).

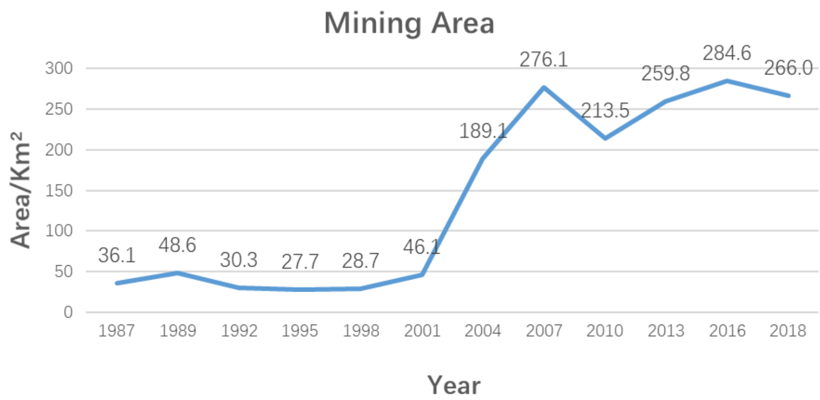

Figure 15. The mining area of Mount Wutai from 1987 to 2018

This paper also discussed the bare soil, farmland and grass land (Figure 4). Although some researchers[127,128] thought bared soil is debatable in this kind of research. Mount Wutai area is a single-season crop area, the seasonal effective is significance. thus, the farmland is bared for more than half a year. In addition, the landscape of research area is loess plateau, it is no different between bared soil and bared farmland. Therefore, it is inaccuracy to evaluate the change of bared land by total area. However, this paper provides a method based on remote sensing and spatial-temporal analysis, it focuses on the spatial variation at the pixel level, in other words, despite measure bare soil in such area might be inaccurate, it works at the pixel level. Therefore, it seems increased from 1989 to 1992, but if put it in the spatial level, the variation area is grassland or bared soil, and according the table of GDP and population, it could not be the human activities influence. It shows a seasonal effect. From this point of view, some grassland, farmland (bared farmland, terraced fields) and bare soil are changing each other frequently in the study area. Therefore, it is inaccurate to describe the change of themselves. Overall, bared soil and farmland together show an increasing tendency. The grassland tends to degrade. Water in Mount Wutai keeps stable.

4.2 Comprehensive heritage threats assessment index

Disturbances in specific area are complex and interaction drastically, those disturbances sometimes show synergistic effects to environment, on the contrary they are antagonism. For disturbance itself, some are positive to the environment, whereas others are disturbances. Focusing on Mount Wutai, the changes and influence of those four main disturbances can be identified directly, however, it is unknown how it works if put them together. The comprehensive heritage threats assessment index can explain it well despite some drawbacks of this index. Based on comprehensive heritage threats assessment index mentioned in the methodology, 12 phases CHATI from 1987 to 2018 has been generated (Figure 16). In this map, the deep red color stand for extreme high threats and the deep green stands for extreme safety.

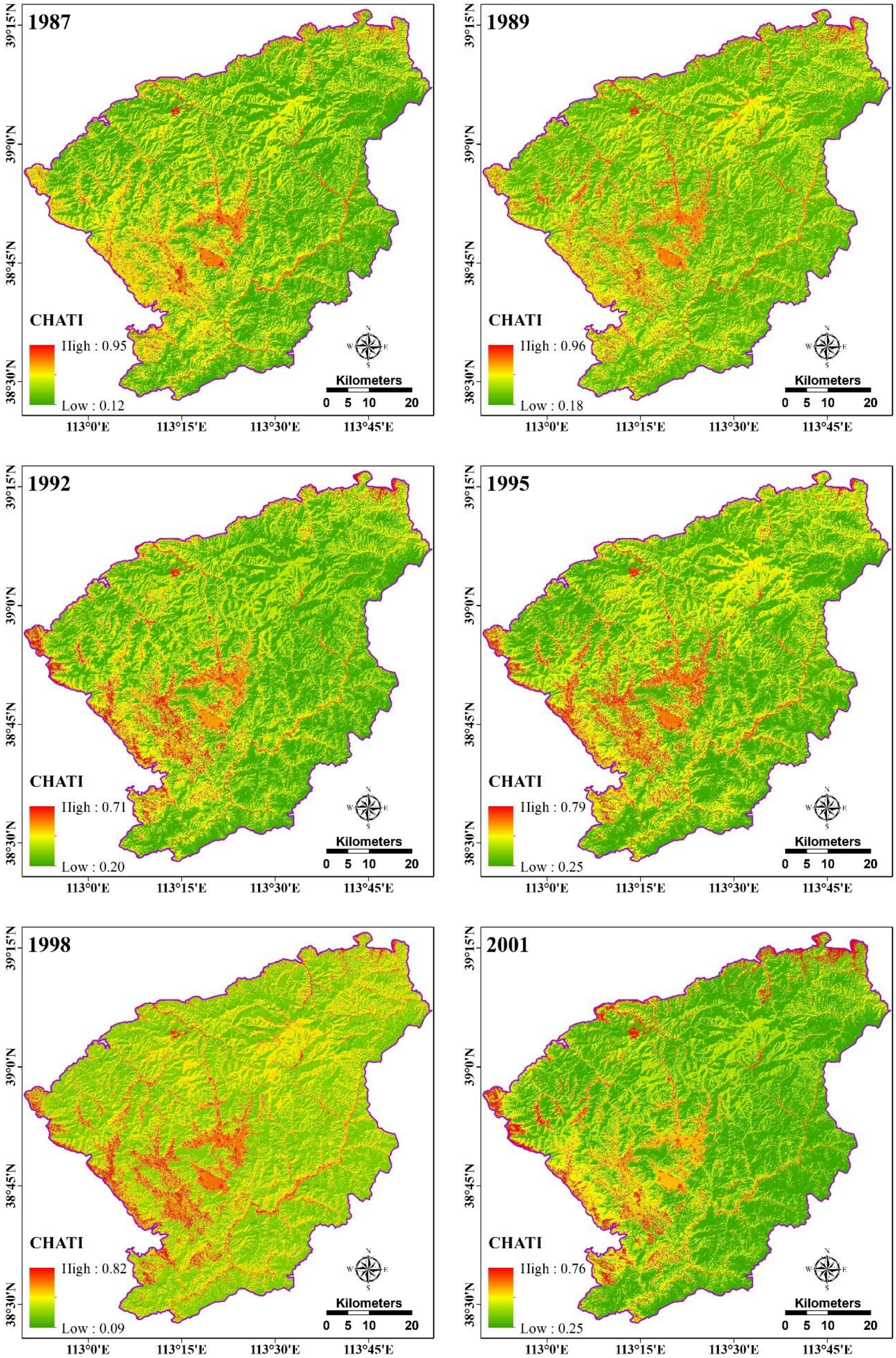
1987
CHATI
High : 0.95
Low : 0.12
1989
CHATI
High : 0.96
Low : 0.18
1992
CHATI
High : 0.71
Low : 0.20
1995
CHATI
High : 0.79
Low : 0.25
1998
CHATI
High : 0.82
Low : 0.09
2001
CHATI
High : 0.76
Low : 0.25
Kilometers
0 5 10 20
39°15'N
39°0'N
38°45'N
38°30'N
113°0'E
113°15'E
113°30'E
113°45'E

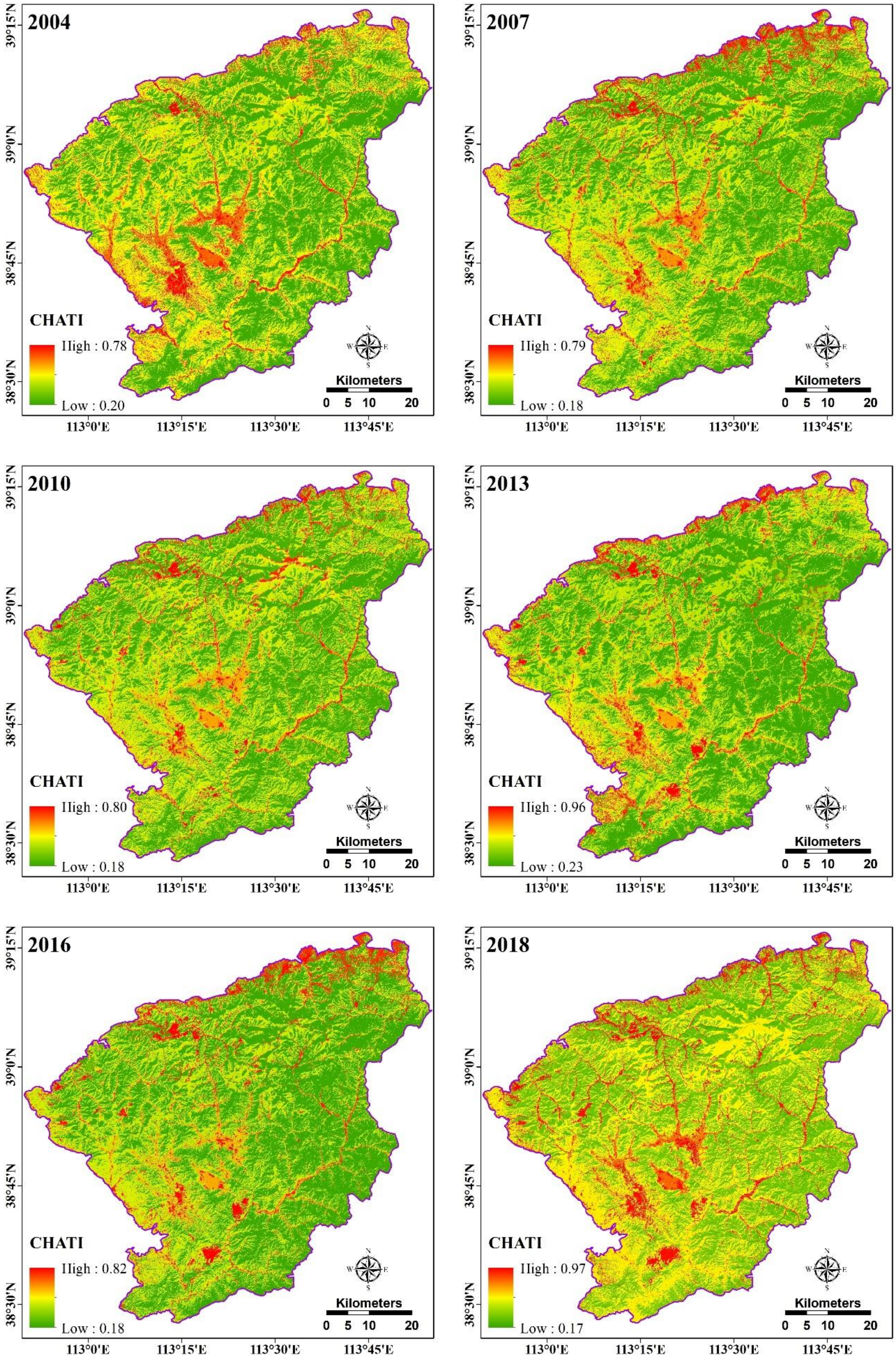

Figure 16. The CHATI from 1987 to 2018

To identity the accuracy of CHATI, research team selected the most recent CHATI map and do the field validation. In the CHATI map of 2018, most of the threatened areas are located in the north part, northwest part and southwest part of Mount Wutai. Through the field works, it is found that the high threaten area in the north part of Mount Wutai is the hematite and magnetite producing region, so there are huge human activities at the foot of the mountain. For instance, the mountain is blasted to take minerals and the crude ores has been crushed and levitated. During the whole process, it produces a large number of tailings. At the same time, although they are legal mining area, due to the poor management in that area, there are visible tailings pond scattered all over the mountain. There is a long history of hematite mines as well in the northeast named Shanyangping. Focus on the southwest of Mount Wutai, there are two open basins, located in Doucun Town and Rucun Town, which are mainly used for agricultural production. Theoretically, farmland should not contribute high threats to the environment, however, as this paper mentioned above, farmland in this area shows a significance seasonal effective (see this area in different year maps based on Figure 16), more than half a year area bared farmland. It pushes a high land stress to the environment. Wutai County, the largest built-up area in the study area, is also located there. There are two open-pit mines around Wutai County. Although it has been closed since 2016, it had been continuously expanding for the past three decades. This area also contributes a large number of threat disturbances to the entire study area. Figure 17 is the map combined CHATI map with fieldwork images.

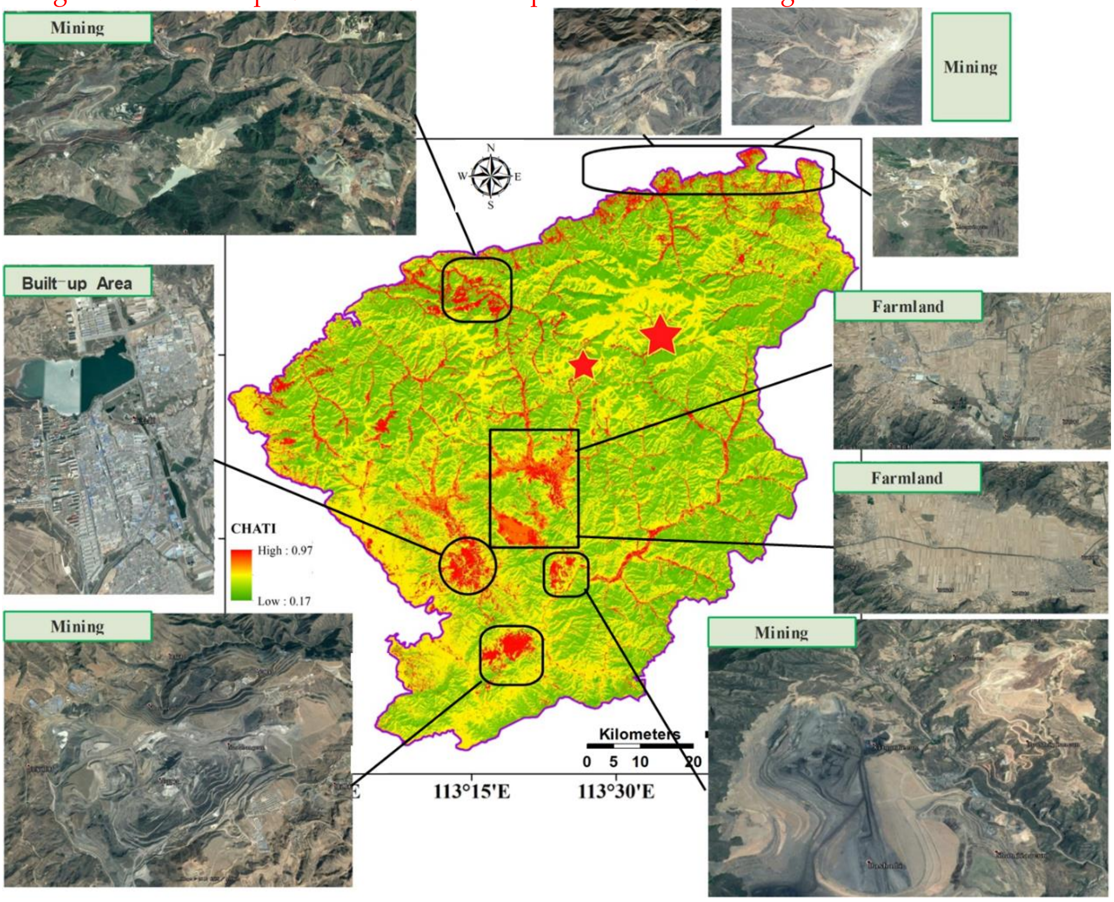

Figure 17. The threat disturbance spatial distribution based CHATI in 2018

To illustrate the spatial-temporal variation of the CHATI during the last 3 decades, based on the linear regression and F-test which mentioned in the methodology, the θ_{slope} and F maps has been derived (Figure 18). If θ_{slope} is positive, it indicates that the research object changes with time, and the larger the value, the more obvious the upward trend; otherwise, the research object declines. The interannual rate of change (Slope value) of Mount Wutai from 1987 to 2018 ranges from -0.047 to 0.057. The obvious changes of the research area are located in the three part. Firstly, the Wutai Town and the surrounding villages, there is a significance change in θ_{slope} map and display 'significance decrease' in the F map, because the rapid urbanization and economic development driving a large number of built-up areas has been built. Secondly, the bared soil and farmland in the southwest display positive in the θ_{slope} map and 'increase' in the F map, after reviewed each selected year's LULC maps and investigated the local residents around there, there are no significance changes during those years. But a lot of farmland change between abandoned and redevelopment, combined with seasonal effective, led to the significance change this area. That is one of the drawbacks of this research. Thirdly, it concentrate in the northeast of map which is core protect area of Mount Wutai, it display positive in the $\boldsymbol{\theta_{slope}}$ map and 'significance increase' in the ***F*** map, according to the documents[119], during 2000 to 2009 Mount Wutai development rapidly, after that local government leaded a resettlement plan to protect the core culture landscape. Demolition a lot house and rebuilt serval settlement village around the core protect area. That makes such large and continuous changes. Overall, the comprehensive risk of Wutai Mountain is mostly stable.

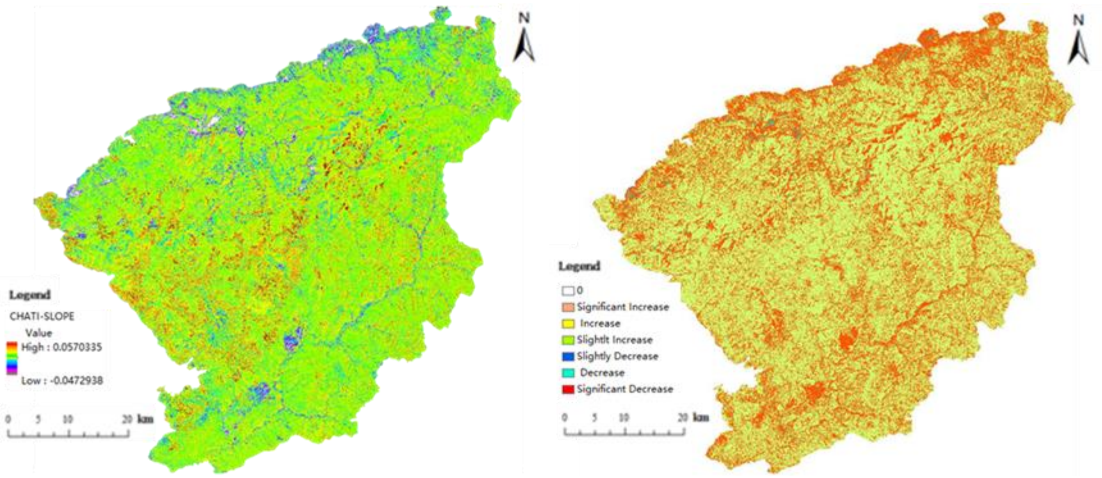

Figure 18. The spatial distribution of the variation trend of CHATI value 1987-2018 in Mount Wutai

5. Conclusion

This research uses multi-source (Landsat, Modis vegetation products and ASTER-DEM) time-series remote sensing data to identify the threats of the Mount Wutai world landscape heritage area. Firstly, LULCC and disturbances of Mount Wutai has been addressed with the human activities. It shows the forest coverage of Mount Wutai has declined compared to 30 years ago, despite the local government has implemented several programme to protect the forest and plant trees, but it still cannot fulfil the deficit of forest which destroyed in the middle term. However, the forest coverage is turn to increase in recent years. The most significance change is the built-up area, especially during 1998 to 2004, the total area of built-up area is doubled. At the same time, due to the high demand of energy market and rapid economic development, the total mining area is increased fivefold. Those dramatically increase direct led to high land stress in the regional level. Secondly, this research proposed a Comprehensive Heritage Area Threats Index (CHATI), this method uses four key normalized indexes constructed a comprehensive system to assessment the threats of entire WHA. The accuracy test based on field validation has proved this framework works, but there are some drawbacks. Based on the result, five high threats area has been investigated, and find out the area is high consist with the LULCC, from this point of view, the CHATI proposed an efficient way to measure the threats of WHA. Thirdly, the linear regression and F-test has adopted in this research to analysis the remarkable characteristics of spatial temporal variation, from the calculation results, the core area of Mount Wutai change dramatically and trend to less threats, on the contrary, the area related built-up area and mining show high threat.

All those results and analysis has been proved reliable and efficient, however, there are some drawbacks need to be discussed here. The time-series Landsat data only use one phases each selected year, although this research try to incorporate same seasonal data, their seasonal effects did not reflect by the result of LULCC and CHATI. At the same time, 30 years 12 phases could model the trend of variation, but it omits some short-term changes. Therefore, dense time-series datasets can solve this problem, but it also leads to a massive amount of computation. Another shortcoming is with respects to the study area, at specific time, bared soil and farmland (abandoned farmland, terraced fields) have same features on remote sensing images and it is hard to differentiate accurately even with DEM, slope and aspect features. This problem can be solved by incorporating free and open remote sensing datasets to extract useful features to better characterise the LULCC. The last disadvantage is the pollution indicator has been ignored for CHATI. In the future, we would include PM2.5, rainfall data etc. to further increase the accuracy and reduce potential uncertainty.

In conclusion, the study shows that there is considerable potential to apply remote sensing and GIS techniques in combination with an assessment system to identify the threat of the World Heritage Area. Long-term time series satellite sensor data could provide rich information to support the WHA monitoring and management. The threat and disturbances are explored that provide a new way to identify and monitor the component of WHA. Indeed, there still have a potential to develop this assessment framework, such as, the classifier method, the data used and the indicators that has been ignored. Hope this research can raise public's awareness on protecting WHA, and provide an efficient tool to guide the public policy making. Finally, we really appreciate to the free and open datasets (Landsat, Modis, Modis vegetation product and ASTER-DEM) to enable us to accomplish such detailed research. Without those datasets, there would be no previous research that we can study. Also, cannot captured the whole research area of Mount Wutai for each selected year.

Author Contributions: Conceptualization, X.B., P.Z. and P.T.; methodology, X.B.; validation, X.B., S.G. and P.D.; formal analysis, X.B.; investigation, S.G., C.L. and P.Z.; data curation, S.G.; writing—original draft preparation, X.B., P.D.; writing—review and editing, S.G., P.D., X.B., P.Z., P.T., C.L., C.Z.; visualization, S.G.; funding acquisition, P.D.;

Funding: This study is supported by Open Research Fund of Key Laboratory of Digital Earth Science, Institute of Remote Sensing and Digital Earth, Chinese Academy of Sciences (GrantNo.2015LDE011), the National Nature Science Foundation of China (GrantNo.41631176). China Scholarship Council Fund and Newton Fund of British Council (File No.201806190301).

Acknowledgments: The authors would like to thank Erzhu Li, Jieqiong Luo, Jike Chen, Hongrui Zheng and Yaping Meng for their help in data process, Ruochen Shang, Zhe Hao, Yun Li and Yaoyao Wang for their help.

Conflicts of Interest: The authors declare no conflict of interest."

References

1. Poria, Y.; Reichel, A.; Cohen, R.J.T.M. Tourists perceptions of World Heritage Site and its designation. **2013**, *35*, 272-274.
2. Drost, A.J.A.o.t.r. Developing sustainable tourism for world heritage sites. **1996**, *23*, 479-484.
3. Leask, A.; Fyall, A. *Managing world heritage sites*; Routledge: 2006.
4. Rössler, M.J.L.R. World heritage cultural landscapes: a UNESCO flagship programme 1992–2006. **2006**, *31*, 333-353.
5. UNESCO. UNESCO World Heritage Centre The criteria for selection. 2011.
6. Agapiou, A.; Lysandrou, V.; Alexakis, D.D.; Themistocleous, K.; Cuca, B.; Argyriou, A.; Sarris, A.; Hadjimitsis, D.G.J.C., Environment; Systems, U. Cultural heritage management and monitoring using remote sensing data and GIS: The case study of Paphos area, Cyprus. **2015**, *54*, 230-239.
7. Cowley, D.C.J. Remote sensing for archaeological heritage management. **2011**.
8. Watson, J.E.M.; Dudley, N.; Segan, D.B.; Hockings, M.J.N. The performance and potential of protected areas. **2014**, *515*, 67-73.
9. Voogt, J.A.; Oke, T.R.J.R.s.o.e. Thermal remote sensing of urban climates. **2003**, *86*, 370-384.
10. Pappu, S.; Akhilesh, K.; Ravindranath, S.; Raj, U.J.J.o.A.S. Applications of satellite remote sensing for research and heritage management in Indian prehistory. **2010**, *37*, 2316-2331.
11. Nagendra, H.; Lucas, R.; Honrado, J.P.; Jongman, R.H.G.; Tarantino, C.; Adamo, M.; Mairota, P.J.E.I. Remote sensing for conservation monitoring: Assessing protected areas, habitat extent, habitat condition, species diversity, and threats. **2013**, *33*, 45-59.
12. Willis, K.S.J.B.C. Remote sensing change detection for ecological monitoring in United States protected

areas. **2015**, *182*, 233-242.

13. RYKIEL JR, E.J.J.A.J.o.E. Towards a definition of ecological disturbance. **1985**, *10*, 361-365.
14. Brimblecombe, P.; Grossi, C.M.; Harris, I. Climate change critical to cultural heritage. In *Survival and sustainability*, Springer: 2010; pp. 195-205.
15. West, P.; Igoe, J.; Brockington, D.J.A.R.A. Parks and peoples: the social impact of protected areas. **2006**, *35*, 251-277.
16. Frey, B.S.; Steiner, L.J.I.J.o.C.P. World Heritage List: does it make sense? **2011**, *17*, 555-573.
17. Gross, J.E.; Goetz, S.J.; Cihlar, J.J.R.S.o.E. Application of remote sensing to parks and protected area monitoring: Introduction to the special issue. **2009**, *113*, 1343-1345.
18. Ali, S.H. *Mining, the environment, and indigenous development conflicts*; University of Arizona Press: 2009.
19. Rice, J.; Trujillo, V.; Jennings, S.; Hylland, K.; Hagstrom, O.; Astudillo, A.; Jensen, J.N.J.C.R.R.-I.C.F.T.E.O.T.S. Guidance on the application of the ecosystem approach to management of human activities in the European marine environment. **2005**, *273*.
20. Xu, X.; Yang, G.; Tan, Y.; Zhuang, Q.; Li, H.; Wan, R.; Su, W.; Zhang, J.J.S.o.t.T.E. Ecological risk assessment of ecosystem services in the Taihu Lake Basin of China from 1985 to 2020. **2016**, *554*, 7-16.
21. Maekawa, M.; Lanjouw, A.; Rutagarama, E.; Sharp, D. Mountain gorilla tourism generating wealth and peace in post‐conflict R wanda. In Proceedings of Natural Resources Forum; pp. 127-137.
22. Kennedy, R.; Yang, Z.; Braaten, J.; Neldon, P.; Cohen, W.J.R.S.o.P.L. Monitoring landscape dynamics of National Parks in the western United States. **2012**, 57-75.
23. Wiens, J.; Sutter, R.; Anderson, M.; Blanchard, J.; Barnett, A.; Aguilar-Amuchastegui, N.; Avery, C.; Laine, S.J.R.S.o.E. Selecting and conserving lands for biodiversity: the role of remote sensing. **2009**, *113*, 1370-1381.
24. Dennison, P.E.; Nagler, P.L.; Hultine, K.R.; Glenn, E.P.; Ehleringer, J.R.J.R.S.o.E. Remote monitoring of tamarisk defoliation and evapotranspiration following saltcedar leaf beetle attack. **2009**, *113*, 1462-1472.
25. Jones, J.W.; Hall, A.E.; Foster, A.M.; Smith, T.J.J.F.E. Wetland fire scar monitoring and analysis using archival Landsat data for the Everglades. **2013**, *9*, 133-150.
26. Munns Jr, W.J.E.; Society. Assessing risks to wildlife populations from multiple stressors: overview of the problem and research needs. **2006**, *11*.
27. Feng, Y.; Liu, Y.; Liu, Y.J.S.E.R.; Assessment, R. Spatially explicit assessment of land ecological security with spatial variables and logistic regression modeling in Shanghai, China. **2017**, *31*, 2235-2249.
28. DeFries, R.; Hansen, A.; Newton, A.C.; Hansen, M.C.J.E.a. Increasing isolation of protected areas in tropical forests over the past twenty years. **2005**, *15*, 19-26.
29. Ingram, J.C.; Dawson, T.P.; Whittaker, R.J.J.R.S.o.E. Mapping tropical forest structure in southeastern Madagascar using remote sensing and artificial neural networks. **2005**, *94*, 491-507.
30. Nunes, M.C.; Vasconcelos, M.J.; Pereira, J.M.; Dasgupta, N.; Alldredge, R.J.; Rego, F.C.J.L.E. Land cover type and fire in Portugal: do fires burn land cover selectively? **2005**, *20*, 661-673.
31. Fuller, D.O.J.S.J.o.T.G. Tropical forest monitoring and remote sensing: A new era of transparency in forest governance? **2006**, *27*, 15-29.
32. Nagendra, H.; Pareeth, S.; Sharma, B.; Schweik, C.M.; Adhikari, K.R.J.L.E. Forest fragmentation and regrowth in an institutional mosaic of community, government and private ownership in Nepal. **2008**, *23*, 41-54.
33. Nagendra, H.; Rocchini, D.; Ghate, R.; Sharma, B.; Pareeth, S.J.R.S. Assessing plant diversity in a dry tropical forest: Comparing the utility of Landsat and IKONOS satellite images. **2010**, *2*, 478-496.

34. Luo, J.; Du, P.; Samat, A.; Xia, J.; Che, M.; Xue, Z.J.S.R. Spatiotemporal Pattern of PM2.5 Concentrations in Mainland China and Analysis of Its Influencing Factors using Geographically Weighted Regression. **2017**, *7*.
35. Du, P.; Xia, J.; Zhang, W.; Tan, K.; Liu, Y.; Liu, S.J.S. Multiple classifier system for remote sensing image classification: A review. **2012**, *12*, 4764-4792.
36. Du, P.; Samat, A.; Waske, B.; Liu, S.; Li, Z.J.I.J.o.P.; Sensing, R. Random forest and rotation forest for fully polarized SAR image classification using polarimetric and spatial features. **2015**, *105*, 38-53.
37. Du, P.; Liu, S.; Xia, J.; Zhao, Y.J.I.F. Information fusion techniques for change detection from multi-temporal remote sensing images. **2013**, *14*, 19-27.
38. Pôças, I.; Cunha, M.; Pereira, L.S.J.A.G. Remote sensing based indicators of changes in a mountain rural landscape of Northeast Portugal. **2011**, *31*, 871-880.
39. Gitelson, A.A.; Merzlyak, M.N.J.J.o.p.p. Signature analysis of leaf reflectance spectra: algorithm development for remote sensing of chlorophyll. **1996**, *148*, 494-500.
40. Liu, Y.; Sarnat, J.A.; Kilaru, V.; Jacob, D.J.; Koutrakis, P.J.E.s.; technology. Estimating ground-level PM2. 5 in the eastern United States using satellite remote sensing. **2005**, *39*, 3269-3278.
41. Van Donkelaar, A.; Martin, R.V.; Park, R.J.J.J.o.G.R.A. Estimating ground-level PM2. 5 using aerosol optical depth determined from satellite remote sensing. **2006**, *111*.
42. Kimes, D.; Sellers, P.J.R.S.o.E. Inferring hemispherical reflectance of the Earth's surface for global energy budgets from remotely sensed nadir or directional radiance values. **1985**, *18*, 205-223.
43. Bastiaanssen, W.G.; Menenti, M.; Feddes, R.; Holtslag, A.J.J.o.h. A remote sensing surface energy balance algorithm for land (SEBAL). 1. Formulation. **1998**, *212*, 198-212.
44. Jackson, T.J.J.H.p. III. Measuring surface soil moisture using passive microwave remote sensing. **1993**, *7*, 139-152.
45. Weng, Q.J.I.j.o.r.s. A remote sensing? GIS evaluation of urban expansion and its impact on surface temperature in the Zhujiang Delta, China. **2001**, *22*, 1999-2014.
46. Gao, B.-C.J.R.s.o.e. NDWI—A normalized difference water index for remote sensing of vegetation liquid water from space. **1996**, *58*, 257-266.
47. Bai, Z.; Dent, D.; Olsson, L.; Schaepman, M. *Global assessment of land degradation and improvement: 1. identification by remote sensing*; ISRIC-World Soil Information: 2008.
48. Curran, P.J.P.i.p.g. Multispectral remote sensing of vegetation amount. **1980**, *4*, 315-341.
49. Lu, D.J.I.j.o.r.s. The potential and challenge of remote sensing-based biomass estimation. **2006**, *27*, 1297-1328.
50. Ruimy, A.; Saugier, B.; Dedieu, G.J.J.o.G.R.A. Methodology for the estimation of terrestrial net primary production from remotely sensed data. **1994**, *99*, 5263-5283.
51. Field, C.B.; Randerson, J.T.; Malmström, C.M.J.R.s.o.E. Global net primary production: combining ecology and remote sensing. **1995**, *51*, 74-88.
52. Lefsky, M.A.; Cohen, W.B.; Parker, G.G.; Harding, D.J.J.B. Lidar remote sensing for ecosystem studies: Lidar, an emerging remote sensing technology that directly measures the three-dimensional distribution of plant canopies, can accurately estimate vegetation structural attributes and should be of particular interest to forest, landscape, and global ecologists. **2002**, *52*, 19-30.
53. Dandois, J.P.; Ellis, E.C.J.R.S. Remote sensing of vegetation structure using computer vision. **2010**, *2*, 1157-1176.
54. Kerr, J.T.; Ostrovsky, M.J.T.i.e.; evolution. From space to species: ecological applications for remote

sensing. **2003**, *18*, 299-305.
55. Quattrochi, D.A.; Luvall, J.C.J.L.e. Thermal infrared remote sensing for analysis of landscape ecological processes: methods and applications. **1999**, *14*, 577-598.
56. Van Donkelaar, A.; Martin, R.V.; Brauer, M.; Hsu, N.C.; Kahn, R.A.; Levy, R.C.; Lyapustin, A.; Sayer, A.M.; Winker, D.M.J.E.s.; technology. Global estimates of fine particulate matter using a combined geophysical-statistical method with information from satellites, models, and monitors. **2016**, *50*, 3762-3772.
57. Zheng, Y.; Zhang, Q.; Liu, Y.; Geng, G.; He, K.J.A.E. Estimating ground-level PM2. 5 concentrations over three megalopolises in China using satellite-derived aerosol optical depth measurements. **2016**, *124*, 232-242.
58. Guo, Y.; Tang, Q.; Gong, D.-Y.; Zhang, Z.J.R.S.o.E. Estimating ground-level PM2. 5 concentrations in Beijing using a satellite-based geographically and temporally weighted regression model. **2017**, *198*, 140-149.
59. Simic, A.; Chen, J.M.; Liu, J.; Csillag, F.J.R.S.o.E. Spatial scaling of net primary productivity using subpixel information. **2004**, *93*, 246-258.
60. Bian, J.-h.; Li, A.; Song, M.; Ma, L.; Jiang, J.J.J.o.R.S. Reconstruction of NDVI time-series datasets of MODIS based on Savitzky-Golay filter. **2010**, *14*, 725-741.
61. Lu, D.; Xu, X.; Tian, H.; Moran, E.; Zhao, M.; Running, S.J.E.M. The effects of urbanization on net primary productivity in southeastern China. **2010**, *46*, 404-410.
62. Xu, H.; Wang, M.; Shi, T.; Guan, H.; Fang, C.; Lin, Z.J.E.i. Prediction of ecological effects of potential population and impervious surface increases using a remote sensing based ecological index (RSEI). **2018**, *93*, 730-740.
63. Srinivasa Rao, Y.; Jugran, D.J.H.S.J. Delineation of groundwater potential zones and zones of groundwater quality suitable for domestic purposes using remote sensing and GIS. **2003**, *48*, 821-833.
64. Miller, R.B.; Small, C.J.E.S.; Policy. Cities from space: potential applications of remote sensing in urban environmental research and policy. **2003**, *6*, 129-137.
65. Luo, J.; Zhou, T.; Du, P.; Xu, Z.J.F.o.E.S. Spatial-temporal variations of natural suitability of human settlement environment in the Three Gorges Reservoir Area—A case study in Fengjie County, China. **2019**, *13*, 1-17, doi:10.1007/s11707-018-0683-2.
66. Yinkang, C.F.L.M.Z.; Feng, Z.J.J.O.N.U. ANALYSIS OF THE SPATIAL DISTRIBUTION PATTERN OF URBAN LAND PRICE WITH GEOSTATISTICS [J]. **1999**, *6*.
67. Luo, J.; Du, P.; Samat, A.; Feng, L. Evaluation on the natural suitability of urban human settlement environment using multisource data. In Proceedings of 2015 Joint Urban Remote Sensing Event (JURSE); pp. 1-4.
68. Patino, J.E.; Duque, J.C.; Pardo-Pascual, J.E.; Ruiz, L.A.J.A.G. Using remote sensing to assess the relationship between crime and the urban layout. **2014**, *55*, 48-60.
69. Xu, Z.; Li, Q.J.H.I. Integrating the empirical models of benchmark land price and GIS technology for sustainability analysis of urban residential development. **2014**, *44*, 79-92.
70. Xu, Y.; Sun, J.; Zhang, J.; Xu, Y.; Zhang, M.; Liao, X.J.I.J.o.G.I.S. Combining AHP with GIS in synthetic evaluation of environmental suitability for living in China's 35 major cities. **2012**, *26*, 1603-1623.
71. Ouzounis, G.K.; Syrris, V.; Pesaresi, M.J.P.R.L. Multiscale quality assessment of Global Human Settlement Layer scenes against reference data using statistical learning. **2013**, *34*, 1636-1647.
72. Shen, L.; Kyllo, J.; Guo, X.J.S. An integrated model based on a hierarchical indices system for monitoring

and evaluating urban sustainability. **2013**, *5*, 524-559.
73. Xu, C.; Liu, M.; An, S.; Chen, J.; Yan, P.J.J.o.e.m. Assessing the impact of urbanization on regional net primary productivity in Jiangyin County, China. **2007**, *85*, 597-606.
74. Wu, C.; Murray, A.T.J.R.s.o.E. Estimating impervious surface distribution by spectral mixture analysis. **2003**, *84*, 493-505.
75. Du, H.; Cai, W.; Xu, Y.; Wang, Z.; Wang, Y.; Cai, Y.J.U.F.; Greening, U. Quantifying the cool island effects of urban green spaces using remote sensing Data. **2017**, *27*, 24-31.
76. Du, P.; Bai, X.; Luo, J.; Li, E.; Lin, C.J.N.X.G.D.X. Advances of urban remote sensing. **2018**, *10*, 16-29.
77. Li, S.; Zhao, G.; Wilde, S.A.; Zhang, J.; Sun, M.; Zhang, G.; Dai, L.J.G.R. Deformation history of the Hengshan–Wutai–Fuping Complexes: implications for the evolution of the Trans-North China Orogen. **2010**, *18*, 611-631.
78. Liu, S.; Pan, Y.; Xie, Q.; Zhang, J.; Li, Q.J.P.R. Archean geodynamics in the Central Zone, North China Craton: constraints from geochemistry of two contrasting series of granitoids in the Fuping and Wutai complexes. **2004**, *130*, 229-249.
79. Stevenson, D.J.R.o.C.i.P. Visions of Mañjuśrī on Mount Wutai. **1996**, *3*, 203.
80. Lin, W.-C. *Building a Sacred Mountain: The Buddhist Architecture of China's Mount Wutai*; University of Washington Press: 2014.
81. Ryan, C.; Gu, H.J.T.m. Constructionism and culture in research: Understandings of the fourth Buddhist Festival, Wutaishan, China. **2010**, *31*, 167-178.
82. Wang, K.; Li, J.; Hao, J.; Li, J.; Shaoping, Z.J.P.R. The Wutaishan orogenic belt within the Shanxi Province, northern China: a record of late Archaean collision tectonics. **1996**, *78*, 95-103.
83. Yearbook. Wutai Bureau of statistics of Wutai county. **2010**.
84. Yearbook. Wutai Bureau of statistics of Wutai County. **2013**.
85. ZHANG, W.; WANG, J.J.J.o.H.U.o.T. School of Tourism Management, Xiangtan University;; On Development of Red Tourism Resources in China——Taking Wutai County in Shanxi Province as an Example [J]. **2013**, *4*.
86. Thenkabail, P.S.; Schull, M.; Turral, H.J.R.S.o.E. Ganges and Indus river basin land use/land cover (LULC) and irrigated area mapping using continuous streams of MODIS data. **2005**, *95*, 317-341.
87. Yang, X.; Huang, Y.; Dong, P.; Jiang, D.; Liu, H.J.S. An updating system for the gridded population database of China based on remote sensing, GIS and spatial database technologies. **2009**, *9*, 1128-1140.
88. Mengistu, D.A.; Salami, A.T.J.A.J.o.E.S.; Technology. Application of remote sensing and GIS inland use/land cover mapping and change detection in a part of south western Nigeria. **2007**, *1*, 99-109.
89. Alo, C.A.; Pontius Jr, R.G.J.E.; Planning, P.B.; Design. Identifying systematic land-cover transitions using remote sensing and GIS: the fate of forests inside and outside protected areas of Southwestern Ghana. **2008**, *35*, 280-295.
90. Liu, J.; Linderman, M.; Ouyang, Z.; An, L.; Yang, J.; Zhang, H.J.S. Ecological degradation in protected areas: the case of Wolong Nature Reserve for giant pandas. **2001**, *292*, 98-101.
91. Kairo, J.G.; Kivyatu, B.; Koedam, N.J.E.D.; Sustainability. Application of Remote Sensing and GIS in the Management of Mangrove Forests Within and Adjacent to Kiunga Marine Protected Area, Lamu, Kenya. **2002**, *4*, 153-166.
92. Running, S.W. Estimating terrestrial primary productivity by combining remote sensing and ecosystem simulation. In *Remote sensing of biosphere functioning*, Springer: 1990; pp. 65-86.
93. Myneni, R.B.; Hall, F.G.; Sellers, P.J.; Marshak, A.L.J.I.T.o.G.; Sensing, R. The interpretation of spectral

vegetation indexes. **1995**, *33*, 481-486.

94. Han-Qiu, X.J.J.o.R.S. A Study on Information Extraction of Water Body with the Modified Normalized Difference Water Index (MNDWI)[J]. **2005**, *5*, 589-595.
95. Zhou, C.-l.; XU, H.-q.J.J.o.I.; Graphics. A Spectral Mixture Analysis and Mapping of Impervious Surfaces in Built-up Land of Fuzhou City [J]. **2007**, *5*, 875-881.
96. Xu, H.J.T.o.t.C.S.o.A.E. Assessment of ecological change in soil loss area using remote sensing technology. **2013**, *29*, 91-97.
97. Xu, h. Fast information extraction of urban built-up land based on the analysis of spectral signature and normalized difference index. *geographical research (in Chinese)* **2005**.
98. Xu, H.J.I.J.o.R.S. A new index for delineating built-up land features in satellite imagery. **2008**, *29*, 4269-4276.
99. Huete, A.R.J.R.s.o.e. A soil-adjusted vegetation index (SAVI). **1988**, *25*, 295-309.
100. Zhu, G.; Liu, Y.; Ju, W.; Chen, J.J.Y.X.-J.o.R.S. Evaluation of topographic effects on four commonly used vegetation indices. **2013**, *17*, 210-234.
101. Technical Specifications for Evaluation of Ecological Environment Conditions. P.R.China, M.o.R.a.E., Ed. 2015.
102. Seber, G.A.; Lee, A.J. *Linear regression analysis*; John Wiley & Sons: 2012; Vol. 329.
103. Lix, L.M.; Keselman, J.C.; Keselman, H.J.R.o.e.r. Consequences of assumption violations revisited: A quantitative review of alternatives to the one-way analysis of variance F test. **1996**, *66*, 579-619.
104. Tripathy, G.; Ghosh, T.; Shah, S.J.I.J.o.R.S. Monitoring of desertification process in Karnataka state of India using multi-temporal remote sensing and ancillary information using GIS. **1996**, *17*, 2243-2257.
105. Seto, K.C.; Kaufmann, R.K.J.L.E. Modeling the drivers of urban land use change in the Pearl River Delta, China: integrating remote sensing with socioeconomic data. **2003**, *79*, 106-121.
106. Johnson, L.; Bosch, D.; Williams, D.; Lobitz, B.J.A.E.i.A. Remote sensing of vineyard management zones: Implications for wine quality. **2001**, *17*, 557.
107. Johnson, B.A.; Iizuka, K.J.A.G. Integrating OpenStreetMap crowdsourced data and Landsat time-series imagery for rapid land use/land cover (LULC) mapping: Case study of the Laguna de Bay area of the Philippines. **2016**, *67*, 140-149.
108. Belgiu, M.; Drăguţ, L.J.I.J.o.P.; Sensing, R. Comparing supervised and unsupervised multiresolution segmentation approaches for extracting buildings from very high resolution imagery. **2014**, *96*, 67-75.
109. Al-Saady, Y.; Merkel, B.; Al-Tawash, B.; Al-Suhail, Q.J.F.-F.O.G. Land use and land cover (LULC) mapping and change detection in the Little Zab River Basin (LZRB), Kurdistan Region, NE Iraq and NW Iran. **2015**, *43*.
110. Cohen, J.J.E.; measurement, p. A coefficient of agreement for nominal scales. **1960**, *20*, 37-46.
111. Thomlinson, J.R.; Bolstad, P.V.; Cohen, W.B.J.R.S.o.E. Coordinating methodologies for scaling landcover classifications from site-specific to global: Steps toward validating global map products. **1999**, *70*, 16-28.
112. Zhang, M. *China's Poor Regions: Rural-Urban Migration, Poverty, Economic Reform and Urbanisation*; Routledge: 2004.
113. Yearbook. Shanxi Bureau of statistics of Shanxi Province. **2018**.
114. Yearbook. Wutai Bureau of statistics of Wutai County. **2005**.
115. Myneni, R.; Tucker, C.; Asrar, G.; Keeling, C.J.J.o.G.R.A. Interannual variations in satellite-sensed vegetation index data from 1981 to 1991. **1998**, *103*, 6145-6160.

116. Ping Wang, Y.; Murie, A.J.U.S. The process of commercialisation of urban housing in China. **1996**, *33*, 971-989.
117. Chen, J.; Guo, F.; Wu, Y.J.H.I. One decade of urban housing reform in China: Urban housing price dynamics and the role of migration and urbanization, 1995–2005. **2011**, *35*, 1-8.
118. Logan, J.R.; Fang, Y.; Zhang, Z.J.H.S. The winners in China's urban housing reform. **2010**, *25*, 101-117.
119. Yearbook. Wutai Bureau of statistics of Wutai County. **2018**.
120. Yearbook. Wutai Bureau of statistics of Wutai County. **2014**.
121. Xue, L.; Wang, M.Y.; Xue, T.J.D.; Change. 'Voluntary'poverty alleviation resettlement in China. **2013**, *44*, 1159-1180.
122. Jianjun, T.J.C.S. Coal mining safety: China's Achilles' heel. **2007**, *3*, 36-53.
123. Cao, X.J.J.o.c.p. Policy and regulatory responses to coalmine closure and coal resources consolidation for sustainability in Shanxi, China. **2017**, *145*, 199-208.
124. Shaowei, G.H.X.Y.H.J.S.o.I.F. World Financial Crisis and Its Impact on China [J]. **2008**, *11*.
125. Zhang, J.; Fu, M.; Geng, Y.; Tao, J.J.E.P. Energy saving and emission reduction: A project of coal-resource integration in Shanxi Province, China. **2011**, *39*, 3029-3032.
126. Xie, H.; Wang, J.; Shen, B.; Liu, J.; Jiang, P.; Zhou, H.; Liu, H.; Wu, G.J.J.o.C.C.S. New idea of coal mining: scientific mining and sustainable mining capacity. **2012**, *37*, 1069-1079.
127. Metternicht, G.; Zinck, J.J.R.s.o.E. Remote sensing of soil salinity: potentials and constraints. **2003**, *85*, 1-20.
128. Fang, B.; Lakshmi, V.J.J.o.h. Soil moisture at watershed scale: Remote sensing techniques. **2014**, *516*, 258-272.